Published in final edited form as:
Neuroscience. 2010 March 17; 166(2): 680–697. doi:10.1016/j.neuroscience.2009.12.053.

Forebrain Projections of Arcuate Neurokinin B Neurons Demonstrated by Anterograde Tract-Tracing and Monosodium Glutamate Lesions in the Rat

Sally J. Krajewski[1], **Michelle C. Burke**[1], **Miranda J. Anderson**[1], **Nathaniel T. McMullen**[2,3], and **Naomi E. Rance**[1,2,3,4]

[1]Department of Pathology, University of Arizona College of Medicine, Tucson, AZ USA

[2]Department of Cell Biology and Anatomy, University of Arizona College of Medicine, Tucson, AZ USA

[3]Department of Neurology, University of Arizona College of Medicine, Tucson, AZ USA

[4]Evelyn F. McKnight Brain Institute, University of Arizona College of Medicine, Tucson, AZ USA

Abstract

Neurokinin B (NKB) and kisspeptin receptor signaling are essential components of the reproductive axis. A population of neurons resides within the arcuate nucleus of the rat that expresses NKB, kisspeptin, dynorphin, NK3 receptors and estrogen receptor α. Here we investigate the projections of these neurons using NKB-immunocytochemistry as a marker. First, the loss of NKB-immunoreactive (ir) somata and fibers was characterized after ablation of the arcuate nucleus by neonatal injections of monosodium glutamate. Second, biotinylated dextran amine was injected into the arcuate nucleus and anterogradely labeled NKB-ir fibers were identified using dual-labeled immunofluorescence. Four major projection pathways are described: 1) Local projections within the arcuate nucleus bilaterally, 2) Projections to the median eminence including the lateral palisade zone, 3) Projections to a periventricular pathway extending rostrally to multiple hypothalamic nuclei, the septal region and BNST and dorsally to the dorsomedial nucleus and 4) Projections to a ventral hypothalamic tract to the lateral hypothalamus and medial forebrain bundle. The diverse projections provide evidence that NKB/kisspeptin/dynorphin neurons could integrate the reproductive axis with multiple homeostatic, behavioral and neuroendocrine processes. Interestingly, anterograde tract-tracing revealed NKB-ir axons originating from arcuate neurons terminating on other NKB-ir somata within the arcuate nucleus. Combined with previous studies, these experiments reveal a bilateral interconnected network of sex-steroid responsive neurons in the arcuate nucleus of the rat that express NKB, kisspeptin, dynorphin, NK3 receptors and ERα and project to GnRH terminals in the median eminence. This circuitry provides a mechanism for bilateral synchronization of arcuate NKB/kisspeptin/dynorphin neurons to modulate the pulsatile secretion of GnRH.

Keywords

estrogen; GnRH; kisspeptin; dynorphin; reproduction; LH

Corresponding Author: Naomi E. Rance, M.D., Ph.D. Professor, Department of Pathology, University of Arizona College of Medicine, 1501 N. Campbell Avenue, Tucson, Arizona 85724, (520) 626-6099, (520) 626-1027 (fax), nrance@email.arizona.edu.

Loss of function mutations in neurokinin B (NKB), the neurokinin 3 (NK3) receptor (the primary NKB receptor) or the kisspeptin receptor (GPR54) result in hypogonadotrophic hypogonadism with absence of pubertal development (Seminara et al., 2003; de Roux et al., 2003; Topaloglu et al., 2009). These studies document an essential role of NKB and kisspeptin receptor signaling in the regulation of the human reproductive axis. A key element of this regulatory circuitry is a group of neurons in the infundibular (arcuate) nucleus of the hypothalamus that expresses NKB, kisspeptin, dynorphin and estrogen receptor α (ERα) mRNA (Rance et al., 1990; Rance and Young, 1991; Rometo et al., 2007; Rometo and Rance, 2008). In postmenopausal women, these neurons are hypertrophied and display increased of levels of NKB and kisspeptin gene transcripts (Rance and Young, 1991; Rometo et al., 2007). We have hypothesized that NKB/kisspeptin/dynorphin neurons in the human infundibular nucleus participate in the hypothalamic circuitry regulating estrogen negative feedback on gonadotropin secretion (Rance and Young, 1991; Rance, 2009).

A homologous group of NKB/kisspeptin neurons has been identified in the arcuate nucleus of the monkey (Abel et al., 1999; Sandoval-Guzmán et al., 2004; Rometo et al., 2007; Ramaswamy et al., 2008), rat (Rance and Bruce, 1994; Burke et al., 2006; Ciofi et al., 2006; Kirigiti et al., 2009), mouse (Navarro et al., 2009) and ewe (Foradori et al., 2006; Goodman et al., 2007). Estrogen-treatment decreases NKB and kisspeptin gene expression in the arcuate nucleus of ovariectomized monkeys (Abel et al., 1999; Rometo et al., 2007), rats (Rance and Bruce, 1994; Danzer et al., 1999, Adachi et al., 2007) mice (Dellovade and Merchenthaler, 2004; Smith et al., 2005) and sheep (Pillon et al., 2003; Smith et al., 2007). Moreover, studies of transgenic knockout mice indicate that the suppressive effect of estrogen on NKB and kisspeptin gene expression (Dellovade and Merchenthaler, 2004; Smith et al., 2005) as well as the inhibition of LH secretion by estrogen are mediated via ERα (Dorling et al., 2003; Couse et al., 2003). Taken together, these studies suggest that NKB/kisspeptin/dynorphin/ERα neurons in the arcuate nucleus participate in the hypothalamic regulation of estrogen negative feedback. In the ewe, arcuate NKB/kisspeptin/dynorphin/ERα/progesterone receptor-expressing neurons have also been implicated in estrogen positive feedback effects for generation of the LH surge (Caraty et al., 1998; Estrada et al., 2006; Smith et al., 2009) and progesterone inhibition of LH pulse frequency (Goodman et al., 2004).

While there is now considerable interest in determining the precise role of arcuate NKB/kisspeptin/dynorphin neurons in the reproductive axis, the projection pathways by which these neurons could influence reproduction or other homeostatic control systems are largely unknown. We have previously mapped the distribution of dual-labeled NKB/dynorphin-immunoreactive (ir) fibers throughout the rat hypothalamus and adjacent regions (Burke et al., 2006). In that study, colocalization of NKB and dynorphin in cell bodies was only identified in the arcuate nucleus, suggesting that the dual-labeled NKB/dynorphin fibers originated from arcuate neurons. However, because we could not exclude the possibility that NKB and dynorphin were colocalized in nuclei other than the arcuate, it could not be stated with certainty that these fibers represented projections from NKB neurons in the arcuate nucleus. In the present study, two additional techniques are used to evaluate the projection pathways of arcuate NKB/kisspeptin/dynorphin neurons. In both experiments, NKB-immunoreactivity was used as a marker for this subpopulation of neurons based on studies showing that virtually all of the NKB neurons in the rat arcuate nucleus coexpress kisspeptin (Kirigiti et al., 2009), dynorphin (Burke et al., 2006; Ciofi et al., 2006) and ERα (Burke et al., 2006). In a first experiment, neonatal injections of monosodium glutamate (MSG) were used to chemically ablate the arcuate nucleus, including the NKB neurons. Quantitative immunohistochemistry was then used to evaluate the loss of NKB-ir fibers in hypothalamic nuclei and adjacent regions of MSG-injected rats relative to control rats. In a second experiment, the anterograde tracer, biotinlyated dextran amine (BDA), was injected into the arcuate nucleus. Dual label immunofluorescence

was then used to verify uptake of BDA into arcuate NKB neurons and determine the location of NKB-ir fibers that were anterogradely labeled with BDA. Portions of these data have been reported in abstract form (Krajewski et al., 2005a; Krajewski et al., 2008).

Experimental Proceudres

Animal protocols were approved by the University of Arizona Animal Care and Use Committee and conformed to National Institutes of Health guidelines. Animals were housed in a temperature and light controlled environment (12:12 light cycle) and provided with food and water *ad libitum*.

Experiment 1: Localization of sites of NKB-ir fiber loss secondary to chemical ablation of the arcuate nucleus by neonatal injections of MSG

Animals—Four timed-pregnant Sprague-Dawley rats were purchased from Harlan Sprague-Dawley (Indianapolis, IN). On postnatal days 2, 4, 6, 8 and 10, female pups (n = 21) received injections (4mg/g b.w., i.p.) of l-glutamic acid monosodium salt (MSG, MP Biomedicals, Aura, Ohio) dissolved in saline (40 mg MSG/ml). Littermate controls (n = 7) received equivolume injections of saline. 6 MSG-injected rats and 1 littermate control rat died in the neonatal period. At three months of age, control and MSG-treated animals were ovariectomized and hormone-replaced to standardize estrogen levels. They were anesthetized with a cocktail (0.6 ml/kg, i.m.) containing Ketamine (33.3 mg/ml), Xylazine (10.7 mg/ml) and Acepromazine (1.3 mg/ml), ovariectomized and implanted subcutaneously with two silastic capsules containing estradiol (each containing 40 μl of 180 mg/ml 17β-estradiol dissolved in sesame oil). The animals were sacrificed after two weeks of estrogen treatment.

Serum Immunoassays—At the time of sacrifice, blood was collected by cardiac puncture for analysis of serum estradiol and LH. Serum was stored at -20 °C until analysis. Sensitive estradiol radioimmunoassay and rat LH immunoradiometric assay were performed by the University of Virginia Center for Research in Reproduction Ligand Assay and Analysis Core Laboratory. The sensitivity of the estradiol assay was 1.2 pg/ml with an intraassay coefficient of variation of 5.6. The sensitivity of the LH assay was 0.04 ng/ml with an intraassay coefficient of variation of 2.6. Two MSG-injected animals with LH levels below the threshold of detection were included in the analysis by assigning values at the lower limit of detection. Student's t-tests were performed to compare group body weights and hormone levels.

Perfusion and Tissue Sectioning—The rats were administered a lethal dose of sodium pentobarbital (0.7 ml, i.p.) and transcardially perfused with 100 ml of heparinized saline followed by 200 ml of 4% paraformaldehyde in 0.1 M phosphate-buffered saline (PBS), pH 7.4. The brains were removed from the skull, post fixed in 4% paraformaldehyde in 0.1 M PBS for 1 hour at 4°C, and then cryoprotected in ascending sucrose solutions (10%, 20% and 30% in 0.1 M PBS) at 4°C. Blocks containing hypothalami were dissected with the aid of a rat brain matrix (ASI instruments, Warren, MI) and frozen coronal sections (40 μm thickness) were cut on a sliding microtome (AO Instrument Co, Buffalo, NY). Sections were stored in cryoprotectant solution (30% w/v sucrose, 1% w/v polyvinylpyrrolidone, 30% v/v ethylene glycol and 50% v/v 0.1M PBS) at -20°C until use (Watson, Jr. et al., 1986). Every 10th section was stained with methylene blue to evaluate the Nissl architecture and match sections to a rat brain atlas (Swanson, 1992). In one MSG-treated animal, neuronal degeneration was only observed in the ventrolateral subdivision of the arcuate nucleus. The remaining animals exhibited degeneration of the ventromedial and ventrolateral subdivisions of the arcuate nucleus, although there was variation in the amount of ablation of the dorsomedial subdivision, a region containing NKB-immunoreactive neurons. Sections of six animals with the most complete ablation of the dorsomedial subdivision and all of the control rats (n = 6) were

processed for immunohistochemistry. All subsequent descriptions in this paper refer to the rats selected for the immunohistochemical procedures.

Immunohistochemistry—We used a polyclonal proNKB antibody (NB300-201, unnumbered lot, Novus Biologicals, Littleton, CO) raised in rabbit against the mouse peptide 2 sequence (P2, amino acids 50-79 of the preprotachykinin B protein). This antibody has been used extensively in previous studies (Krajewski et al., 2005b; Burke et al., 2006). The labeling observed with this antibody closely matched previous descriptions using other P2 antibodies and the detection of preprotachykinin B mRNA by *in situ* hybridization histochemistry (Warden and Young, 1988; Merchenthaler et al., 1992; Lucas et al., 1992; Marksteiner et al., 1992; Rance and Bruce, 1994; Ciofi et al., 1994). Furthermore, the labeling by this antibody was different from the distribution of preprotachykinin A mRNA (Warden and Young, 1988; Rance and Bruce, 1994) indicating no cross-reactivity with the peptide products of the preprotachykinin A gene. Controls included preabsorbtion (peptide provided by Novus Biologicals, 10 μM, 24-hour incubation), incubation of tissue with serum collected from the rabbit before inoculation with the proNKB antigen (serum provided by Novus Biologicals) and exclusion of the primary antibody.

Sections matching plates 17-20, 22, 25-28, 30 and 32 of a rat brain atlas (Swanson, 1992) (Fig 1) were processed for NKB immunoreactivity (ir) with nickel-intensified DAB for visualization. In order to minimize staining variability, matched sections from experimental and control animals were processed simultaneously during the same immunohistochemistry procedure. Briefly, free-floating sections were washed 3 × 10 minutes in 0.1M PBS, pH 7.4, and treated with 0.5% $NaBH_4$ in 0.1 M PBS for 10 minutes, followed by a 20 minute incubation with 0.3% H_2O_2 in 0.1 M PBS. The sections were blocked for 1 hour in 0.1M PBS containing 0.3% Triton X-100 and 3% normal goat serum and then incubated for 48 hours at 4°C with rabbit anti-proNKB antibody (1:5000) diluted in the blocking solution. The sections were rinsed and incubated with biotinylated goat anti-rabbit IgG (1:250, Vector Laboratories, Burlingame, CA) diluted in the blocking solution for 2 hours, followed by the Vectastain Elite ABC kit (Vector Laboratories) for 1 hour. A nickel-intensified DAB reaction (0.5 mg/ml DAB, 0.15% $NiNH_4SO_4$ in 0.1 M PBS) was performed (3 – 5.5 minute reaction time). Sections were then mounted on gelatinized slides, dehydrated and cover slipped.

Representative sections from control and MSG-treated rats were mapped using an image-combining computer microscope equipped with a LUDL motorized stage (LUDL Electronic Products, Hawthorne, NY), a Lucivid miniature CRT and Neurolucida software (Microbrightfield, Williston, VT). Boundaries were outlined using a 4× Plan objective. The location of each NKB-ir somata was marked and NKB-ir fibers were traced at high magnification (40× PlanApo objective). The drawings were imported into CorelDraw (Corel Inc., Mountain View, CA) to generate the final figures. Fiber lengths less than 2.5 μm were not included in these drawings.

Image Analysis—Slides were coded and images were taken with a 20× Nikon Plan Fluor objective (N.A. 0.50) using a Nikon E1000 microscope (Nikon, Tokyo, Japan) equipped with a LUDL motorized stage and a Photometrics Coolsnap FX camera (Roper Scientific, Trenton, NJ). Background corrections were performed before image acquisition. The sections were systematically imaged and the digital photographs were assembled into photomontages. Quantitative analysis was performed using MetaMorph image analysis software (Universal Imaging Corporation, West Chester, PA). Regions of interest were identified with the aid of a rat brain atlas (Swanson, 1992) and adjacent Nissl-stained sections. The Paxinos atlas was also used to define levels of the arcuate nucleus (Paxinos and Watson, 2007). Regions with well-defined borders (OVLT, MnPO, LSv, MPN, RCA, PVN, ARC, ME and DMN) were outlined and analyzed (Fig.1). For large regions or regions with indeterminate borders (MS, MPOA,

LPOA, BNST, AVPV, AHA, PeFLH, Pe and vht), tissue that fell within the boundaries of pre-defined boxes or shapes was analyzed (Fig. 1). Except for the arcuate nucleus and median eminence which were smaller in MSG-treated animals, the total area of regions used for density measurements was not significantly different in size between groups. Within each region of interest, the threshold was optimized to select the NKB-ir fibers. NKB-ir density was calculated as the area covered by NKB-immunoreactivity divided by the total area of tissue within the boundary. Because there were only rare NKB-ir somata identified in regions outside of the arcuate nucleus, cell bodies were not excluded from this analysis. Student's t-tests were performed to compare groups. One-tailed t-tests were used because MSG-ablation of NKB cell bodies in the arcuate nucleus was expected to produce destruction of NKB fibers.

Experiment 2: Anterograde tract-tracing of arcuate NKB-ir neurons in the hypothalamus of the female rat

Anterograde tracer injection—A total of twenty-five, Sprague-Dawley, female rats (250-300 g, approximately 3 months of age) were used for these experiments. Four rats were used to optimize the injection parameters. The rats were anesthetized with the cocktail described above and placed into a stereotaxic device (David Kopf Instruments, Tujunga, CA). A borosilicate glass electrode (O.D. 1.0 mm) containing 10% BDA (M.W. = 10,000, Invitrogen, Carlsbad, CA) in 0.1 M PBS, pH 7.4, was lowered into the arcuate nucleus (2.8 mm posterior to bregma, 0.2 mm lateral from bregma and 9.6-9.9 mm ventral to skull surface). The anterograde tracer, BDA, was delivered via iontophoresis (3μA positive, 9 seconds on/off for 5 minutes) followed by a five minute wait before withdrawing the electrode. The rats were sacrificed 6-7 days after injection. The BDA injection site was visualized on every fifth section throughout the arcuate nucleus using avidin-biotin-horseradish peroxidase histochemistry (Vectastain Elite ABC Kit). Four rats with BDA injections into the arcuate nucleus were used for mapping dual-labeled NKB/BDA-ir fibers (below). In the remaining rats, the injections were located in the ventromedial nucleus (4), lateral hypothalamus (2), dorsomedial nucleus (1), pial surface, (2), third ventricle (5) or the injection site was not found. Sections from these animals were not processed further.

Dual-label Immunofluorescence—Dual-label immunofluorescence was used to visualize BDA in NKB-ir cell bodies and fibers. The proNKB antibody (described above) was combined with a polyclonal goat anti-biotin antibody (SP 3000, lot number P0710, Vector Laboratories) for visualization of BDA. There was no specific labeling when the goat anti-biotin antibody was used in identical immunohistochemical procedures from rats without BDA injections. In addition, no labeling was observed when this antibody was excluded from the immunohistochemistry procedures.

Free-floating sections were washed in 0.1 M Tris buffer (12.12 g Tris-HCl, 2.78 g Tris base, pH 7.6, Sigma, St Louis, MO) and blocked for 1 hour in a Tris solution containing 0.1% Triton X-100 (Sigma) and 3% normal donkey serum (Millipore, Temecula, CA) in 0.1 M Tris buffer. Unless noted, all subsequent incubations were also performed in Tris solution. Sections were incubated overnight at room temperature with the primary antibodies (rabbit anti-proNKB, 1:5000 and goat anti-biotin, 1:10,000). They were then washed and incubated over a second night with secondary antibodies, donkey anti-rabbit conjugated to Alexa Fluor 488 and donkey anti-goat conjugated to Alexa Fluor 568 (1:10,000, Invitrogen). To aid in the identification of brain regions, sections were washed and incubated for 15 minutes with a nuclear counter-stain (0.3 μM DAPI in 0.1M Tris buffer, Invitrogen). Finally, sections were washed with Tris buffer, mounted on Superfrost plus slides (Fisher Scientific, Pittsburgh, PA), dried and cover-slipped using the Pro-Long Antifade Kit (Invitrogen). Slides were protected from light and stored at -20°C until examination by fluorescent microscopy.

Microscopic Analysis—Every third section through the injection site in the arcuate nucleus was used to verify the uptake of BDA in NKB cell bodies (10-12 sections per animal). For mapping of dual-labeled NKB/BDA-ir fibers, sections were matched to plates in a rat brain atlas as described above. Sections were analyzed using a Nikon E1000 microscope equipped with a VFM epifluorescent attachment, a motorized stage, a Uniblitz model VMM-D1 shutter driver (Vincent Associates, Rochester, NY) and a Photometrics Coolsnap FX camera. Specific filter cubes were used for the visualization of Alexa Fluor 488 (EX: 480/30 nm, DM: 505 nm, BA: 535/40 nm), Alexa Fluor 568 (EX: 560/40, DM: 595, BA: 630/60) and DAPI (EX: 360/40, DM: 400, BA: 460/50) fluorescence.

For identification of single and dual-labeled cells and fibers, digital images of the sections were taken in a systematic step-wise fashion using a 20× Nikon Plan Fluor objective (N.A. 0.50) and the filter sets for each fluorochrome. The images from each section were color-combined and assembled into montages using MetaMorph imaging software. These photomontages were systematically examined to study the distribution of immunoreactivity and identify regions of potential colocalization. Dual-labeled cells and fibers were confirmed using the fluorescent microscope with a 40× Nikon Plan Fluor objective (N.A. 0.75). Because of the density of labeling, sections of the arcuate nucleus and median eminence were also examined throughout the thickness of the section using stacked images (optical axis step size 1.5 μm) and the 40× objective. Cells and fibers were considered double-labeled when the structure could be clearly identified in the same focal plane with each of the filter sets. After confirmation, the photomontages were magnified to allow tracing of dual-labeled cells and fibers using the MetaMorph drawing tools. To confirm close apposition between NKB/BDA axons and NKB-ir cell bodies within the arcuate, images with focal planes of 0.8 μm thickness were captured throughout the cell of interest using a Zeiss LSM 510 NLO confocal microscope (Carl Zeiss, Jena, Germany) equipped with a 100× Plan Apochromat oil immersion objective (N.A. = 1.4). For color illustrations, images were imported into Adobe Photoshop for adjustment of brightness and contrast. The figures were assembled and labeled using Corel Draw Software.

Results

Ablation of the arcuate nucleus by neonatal injection of MSG decreases the density of NKB immunoreactive fibers in the arcuate nucleus, median eminence and multiple regions in the hypothalamus and adjacent areas

The MSG-treated animals exhibited stunted growth, obesity, ovarian atrophy and extensive destruction of the arcuate nucleus in agreement with previous studies (Nemeroff et al., 1978; Clemens et al., 1978; Meister et al., 1989). The MSG-treated animals were smaller (body weight at three months of age: control: 276.2 ± 5.8 g, n = 6; MSG: 193.7 ± 2.4 g, n = 6, mean ± SEM, $p < 0.001$) and had a disproportionate amount of body fat at the time of ovariectomy. In addition, MSG-treatment reduced ovarian weight at 3 months of age (control: 81.6 ± 4.3 mg, n = 6; MSG: 44.1 ± 6.6 mg, n = 6, mean ± SEM, $p < 0.001$) and serum LH at the time of sacrifice (control: 0.44 ± 0.1 ng/ml, n = 6; MSG: 0.06 ± 0.01 ng/ml, n = 6, mean ± SEM, $p < 0.01$). Ovariectomy and estradiol replacement in adult animals resulted in proestrous levels of serum estrogen that were not significantly different between groups at the time of sacrifice (control: 39.7 ± 3.0 pg/ml, n = 5; MSG: 57.3 ± 10.1 pg/ml, n = 3, mean ± SEM).

Nissl-stained sections from the MSG-treated rats revealed extensive loss of cells at anterior, middle and posterior levels of the arcuate nucleus (Fig. 2A and B). As a result of this cell loss, the ventromedial nucleus appeared to be shifted medially and ventrally. In all animals, the arcuate nucleus was relatively preserved at the level of the premammillary arcuate nucleus (Fig. 3 and 4D) as described in previous studies (Seress, 1982). In the MSG-treated animals, the median eminence was generally thinner and the optic nerves, optic chiasm and optic tracts

were reduced in size. In addition to the arcuate nucleus ablation, Nissl-stained sections revealed cell loss in the AVPV in MSG-treated animals.

In control animals, the greatest numbers of NKB-ir cell bodies and fibers were observed within the arcuate nucleus (Figs. 4C and 4D). The NKB-ir cell bodies were identified in all three subdivisions of the arcuate nucleus. Small numbers of NKB-ir cell bodies were also identified in the preoptic area, bed nucleus of the stria terminalis and anterior hypothalamus. A dense network of beaded NKB-ir fibers was identified within the arcuate nucleus extending to the median eminence (Fig. 4C). Branching of NKB-ir fibers was identified within both the arcuate nucleus and the median eminence.

Beaded NKB-ir fibers could be followed from the arcuate nucleus dorsally and rostrally to a periventricular projection pathway in control animals (Fig. 4). From the periventricular projection pathway, fibers could be traced to the dorsomedial nucleus, the parvocellular paraventricular nucleus, the anteroventral periventricular nucleus, median preoptic nucleus and medial preoptic nucleus. At the level of the retrochiasmatic region and the optic chiasm, NKB-ir fibers were identified below the third ventricle (Fig. 4B). Rostrally, NKB-ir fibers were also identified in the medial and lateral portions of the preoptic area, the septum and bed nucleus of the stria terminalis (Fig. 4). A prominent pathway was identified from the periventricular hypothalamus extending dorsally and laterally to the ventral aspect of the lateral septal region (Fig. 4A). Another projection pathway exited the arcuate nucleus ventrolaterally at the base of the brain adjacent to the pial surface. NKB-ir fibers in this ventral hypothalamic pathway extended to the lateral hypothalamic area, the perifornical region and the medial forebrain bundle immediately dorsal to the optic tract (Fig. 4C). Branching of NKB-ir fibers was identified in the retrochiasmatic region, dorsomedial nucleus and ventral lateral septal region. No NKB-ir fibers were identified in the ventromedial, the suprachiasmatic and the supraoptic nuclei.

The MSG-treated rats exhibited virtually complete loss of NKB-ir neurons at most levels of the arcuate nucleus (Figs. 2 and 4C). However, there was preservation of NKB-ir cell bodies caudally in the premammillary arcuate (Fig. 3 and 4D). The small numbers of NKB-ir neurons in the preoptic area, bed nucleus of the stria terminalis and anterior hypothalamus were not affected by MSG treatment. At the levels of the arcuate where the NKB-ir cell bodies were lost, there was nearly complete depletion of NKB-ir fibers in the arcuate nucleus and adjacent median eminence (Figs. 2F and 4C). The density of NKB-ir fibers was also markedly reduced in the periventricular zone of the hypothalamus and the fiber tracts at the ventral surface of the brain.

Quantitative analysis revealed a significant reduction in NKB-immunoreactivity in MSG-treated animals throughout most levels of the arcuate nucleus and adjacent median eminence (Fig. 5A, n = 4-6 rats/group). There was also a significant decline in the density of NKB-ir fibers in the periventricular hypothalamus and ventral hypothalamic tracts (n = 5-6 rats/group). Rostrally, NKB-ir fiber density was significantly reduced in the OVLT, median preoptic nucleus, medial preoptic area, BNST, anterior periventricular region including the AVPV, ventral portion of the lateral septal region and medial preoptic nucleus (n = 3-6 rats/group). There was also a significant decrease in fiber density in the retrochiasmatic area, paraventricular nucleus and dorsal medial nucleus (Fig. 5B). NKB-immunoreactivity was reduced in the premammillary arcuate, posterior median eminence, medial septal region, lateral preoptic area, anterior hypothalamic area and lateral hypothalamic area, but these changes were not significantly different (Fig. 5B).

Anterograde tract-tracing reveals projections of arcuate NKB neurons within the arcuate nucleus bilaterally, to the median eminence and to multiple regions in the hypothalamus and adjacent areas

Injections of BDA into the arcuate nucleus of four rats were identified using avidin-biotin-horseradish peroxidase histochemistry (Fig. 6). These animals had numerous BDA-labeled somata in the arcuate nucleus at the site of injection. In one animal (R24), the injection was midline and labeled arcuate neurons on both sides of the ventricle. Another animal (R10) exhibited BDA-labeled neurons in the adjacent ventromedial nucleus, an area devoid of NKB-ir cell bodies. Examination of every third section through the injection site (10-12 sections/rat) revealed uptake of BDA in a small number of arcuate NKB-ir neurons (4 ± 0.4 NKB/BDA-ir neurons/rat, mean ± SEM, Fig. 7, B-D). There were a few BDA-ir neurons identified outside of the injection site, but none of these were immunoreactive for NKB.

Dual-labeled NKB/BDA-ir axons were the most numerous in the arcuate nucleus on the side of the injection (Fig. 7A). In two of the animals (R10 and R24), NKB/BDA-ir axons were identified throughout the rostral-caudal extent of the arcuate nucleus. In the other two animals, NKB/BDA-ir axons were identified in the arcuate nucleus sections approximately 250 and 350 μm distal from the injection site. Within the arcuate nucleus of three animals (R10, R24 and R29), NKB/BDA-ir axons were identified in close apposition to single-labeled NKB-ir somata and dendrites (Fig. 8). Confocal microscopy confirmed that the contacts between anterogradely-labeled NKB axons and NKB-ir cell bodies within the arcuate nucleus were within a single optical plane.

Numerous beaded NKB/BDA axons could be followed from the arcuate nucleus into the median eminence. Within the median eminence, NKB/BDA axons were traced to the external zone including the lateral palisade zone (Fig. 7). Segments of NKB/BDA fibers were also identified in the median eminence running parallel to the floor of the third ventricle across the internal zone to the opposite side. In two of the three animals with unilateral injections (R10, R27), NKB/BDA-ir axons were identified within the contralateral arcuate nucleus (Fig. 7). In rat R10, close apposition of NKB/BDA-ir axons was observed on NKB-ir cell bodies both ipsilateral and contralateral to the side of injection. In addition to the extensive projections within the arcuate nucleus and median eminence, numerous NKB/BDA axons were identified throughout the periventricular and ventral hypothalamic tracts. Dual-labeled fibers (1-5 NKB/BDA fibers/area in each section) were identified in many areas of the hypothalamus and adjacent regions (Table 1 & Fig. 9).

Single-labeled BDA-axons were identified in the regions described for dual-labeled fibers, as well as the OVLT, retrochiasmatic area, anterior hypothalamus, ventromedial, suprachiasmatic and supraoptic nuclei. These data are consistent with previous tract-tracing studies of arcuate neurons (Chronwall, 1985; Bouret et al., 2004, Simerly, 2004). Numerous single-labeled BDA fibers were identified in close apposition to NKB-immunoreactive neurons both ipsilateral and contralateral to the injection site.

Extensive numbers of single-labeled NKB-ir fibers were identified, most prominently in the arcuate nucleus, median eminence, the periventricular and ventral hypothalamic tracts, medial preoptic area, ventral lateral septum, paraventricular nucleus and dorsomedial nucleus. The localization of NKB neurons and fibers using immunofluorescence was consistent with the NKB-immunoreactivity described in the MSG control animals (Fig. 4).

Discussion

Current studies indicate that NKB, the NK3 receptor and the kisspeptin receptor (GPR54) are essential components of the reproductive axis (Seminara et al., 2003; de Roux et al., 2003;

Topaloglu et al., 2009). A group of sex-steroid responsive neurons exists within the human infundibular nucleus that expresses NKB, kisspeptin and dynorphin mRNA (Rance and Young, 1991; Rometo et al., 2007; Rometo and Rance, 2008). In the present study, the projections of a homologous group of neurons in the female rat was examined using MSG ablation of the arcuate nucleus and anterograde tract-tracing with NKB-immunoreactivity as a marker. We describe four projection pathways of arcuate NKB/kisspeptin/dynorphin neurons in the rat (Fig. 10): 1) Local projections within the arcuate nucleus (including to other arcuate NKB-ir neurons) and across the median eminence to the contralateral arcuate; 2) Projections to the internal and external zones of the median eminence; 3) Projections within a periventricular pathway extending rostrally to multiple nuclei including the paraventricular nucleus, AVPV, preoptic region, medial preoptic nucleus, median preoptic nucleus, septal nuclei and BNST, dorsally to the dorsomedial nucleus and caudally to the ventral premammillary nucleus; 4) Projections to a ventral hypothalamic tract passing within the lateral hypothalamus and medial forebrain bundle.

Since its description in 1969, MSG-treatment of neonatal animals has been used to study the function and projections of arcuate neurons (Olney, 1969). This treatment results in degeneration of neurons in the arcuate nucleus with some preservation of the dorsomedial subdivision, but spares fibers en passage (Meister et al., 1989).

Interestingly, we observed that the AVPV degenerated in MSG-treated animals. Because the AVPV is an important additional site of kisspeptin cell bodies in the rodent (Smith et al., 2005; Clarkson et al., 2008), this factor would severely limit the usefulness of MSG-treatment for evaluating kisspeptin-ir projections from the arcuate. However, destruction of the AVPV was not considered to be a serious limitation in the present study because NKB-ir cell bodies are not located in the AVPV. NKB-ir neurons were preserved in the arcuate nucleus at the level of the ventral premammillary nucleus and there were also a few NKB-ir neurons preserved in the dorsomedial subdivision of the arcuate nucleus in our animals. Importantly, MSG-treatment did not destroy NKB-ir neurons in other regions of the basal forebrain, such as the BNST, POA and AHA. Preservation of NKB-ir cells in the premammillary arcuate nucleus or elsewhere may explain why the fiber density was reduced, but not significantly, in a few regions shown to receive arcuate NKB-ir projections by the other methods (Fig. 10).

MSG-treatment produces a complicated phenotype, in which animals are stunted, obese, hypogonadal and have low serum levels of growth hormone, thyroid hormone and gonadal steroids (Nemeroff et al., 1978; Clemens et al., 1978; Meister et al., 1989). Because NKB gene expression in the rat arcuate nucleus is strongly modulated by estrogen (Rance and Bruce, 1994; Danzer et al., 1999), the rats in the present study were ovariectomized and estradiol-replaced to standardize estrogen levels. However, we cannot exclude the possibility that other changes in the hormonal environment could have altered the detection of NKB-ir neurons or fibers. In agreement with previous studies (Clemens et al., 1978; Badger et al., 1982), serum LH was significantly lower in the MSG-treated animals. Although there are reports of normal pulsatile LH secretion (Badger et al., 1982) and preserved estrogen negative feedback (Greeley, Jr. et al., 1978) after MSG-treatment, these experiments did not perform histological examination of the arcuate nucleus. In the present study, we observed preservation of the NKB-ir neurons in the posterior arcuate nucleus and variable loss in the dorsomedial subdivision, another site of NKB neurons. These data indicate the importance of determining the extent of arcuate nucleus degeneration before interpreting the results of MSG-experiments.

Anterograde tract-tracing was performed using BDA, a sensitive and reliable agent that can be iontophorectically injected in very small quantities. BDA (10,000 MW) is taken up by neurons at the site of injection and transported along their axons to reveal their projection sites (Reiner et al., 2000). Combined with dual-label immunofluorescence, this technique allows the tract-

tracing of peptidergic neurons with high specificity. A potential confounding factor of this method is retrograde labeling of cell bodies with subsequent anterograde labeling of axon collaterals (Reiner et al., 2000). This was not a significant issue in the present study because only rare BDA-labeled cell bodies were identified outside of the injection site and none of these neurons were NKB-positive. A limitation is that only a small number of NKB-ir neurons took up BDA at the site of injection, and thus, there were only small numbers of dual-labeled fibers identified in each of the brain areas. This paucity of labeling may explain why there was some variation in the detection of NKB/BDA-ir fibers between animals. Despite this limitation, our results are in agreement with previous descriptions of arcuate nucleus projections that were not chemically characterized (Chronwall, 1985; Bouret et al., 2004; Simerly, 2004). Moreover, the anterograde-tract tracing results were complementary to the MSG-experiment and location of the NKB/dynorphin-ir fibers (Burke et al., 2006). Although each technique has limitations, the combination of these three methods allows for a more complete understanding of the projections of arcuate NKB/kisspeptin/dynorphin neurons (Fig. 10).

The present study provides compelling evidence that arcuate NKB/kisspeptin/dynorphin neurons project extensively within the arcuate nucleus. At the levels where MSG-treatment resulted in degeneration of arcuate NKB-ir neurons, there was virtually complete loss of the dense network of NKB-ir fibers. These data agree with the preservation of NKB-ir fibers in the arcuate nucleus after isolating this nucleus from the rest of the brain by knife cuts (Ciofi et al., 2006). Moreover, BDA injection into the arcuate nucleus resulted in numerous anterogradely-labeled NKB axons in sections of the arcuate nucleus distant from the injection site. Segments of NKB/BDA axons could also be traced from the arcuate nucleus to the internal zone of the median eminence, and across the median eminence to the arcuate nucleus on the opposite side. These data provide the first description of arcuate NKB-ir neurons projecting bilaterally within the arcuate nucleus.

Our studies also provide further documentation of communication between NKB-ir neurons within the arcuate nucleus. In particular, injections of BDA into the arcuate nucleus resulted in anterograde labeling of NKB-ir axons terminating on single-labeled arcuate NKB-ir neurons. These data are consistent with the previous descriptions of close apposition of dual-labeled NKB/dynorphin-ir axons on NKB/dynorphin cell bodies and dendrites within the arcuate nucleus (Burke et al., 2006). There is also strong evidence of communication between NKB/kisspeptin/dynorphin/ERα/progesterone receptor-expressing neurons in the arcuate nucleus of the ewe (Foradori et al., 2006). Communication among arcuate NKB/kisspeptin/dynorphin neurons is likely to be mediated, at least in part, by NKB, as the NK3 receptor protein or its mRNA is expressed on these neurons in the rat (Burke et al., 2006), mouse (Navarro et al., 2009) and ewe (Amstalden et al., 2009). Interestingly, Golgi studies in the rat have shown bifurcation of axons originating from arcuate neurons with collaterals terminating locally and other branches entering the median eminence (Van den Pol and Cassidy, 1982). In this study, we also identified branching of beaded NKB-ir axons within the arcuate nucleus and median eminence. Thus, a single NKB neuron could give rise to collaterals that synapse with other arcuate NKB neurons, as well as other branches that project to the median eminence and the arcuate nucleus on the opposite side.

MSG-induced depletion of arcuate NKB-ir neurons was accompanied by near-complete loss of the numerous NKB-ir axons in the adjacent median eminence. These data indicate that most (if not all) of the NKB-ir axons within the median eminence originate from the arcuate nucleus. The loss of NKB axons was not secondary to a nonspecific disruption of the median eminence because GnRH axons are preserved in MSG-treated animals (Jennes et al., 1984; Meister et al., 1989). Furthermore, BDA injections into the arcuate nucleus resulted in anterograde labeling of NKB-ir axons in both the internal and external zones of the median eminence, including the lateral palisade zone, a site with dense GnRH terminals. Although our studies

indicate that arcuate NKB neurons project to the median eminence, they are not labeled by the retrograde tracer, Fluorogold, after systemic injection (Krajewski et al., 2005b). Thus, unlike neurons that secrete hypophysiotrophic hormones, these neurons do not appear to terminate on the fenestrated capillaries of the portal system. However, arcuate NKB neurons may modulate LH secretion through interactions with GnRH terminals in the median eminence, rather than direct effects on pituitary gonadotrophs. NKB and GnRH axons are closely apposed within the median eminence of the rat (Krajewski et al., 2005b) and ultrastructural studies have confirmed direct contact of NKB varicosities with GnRH axons without a synapse (Ciofi et al., 2006). GnRH neurons in the mouse express NK3 receptor mRNA (Todman et al., 2005) and there is extensive colocalization of NK3 receptor protein on GnRH terminals in the median eminence of the rat (Krajewski et al., 2005b). Therefore, projections of arcuate NKB neurons to the median eminence could modulate GnRH secretion via non-synaptic transmission via the NK3 receptor (Merighi, 2002).

Taken together with previous studies (described above), these experiments reveal a bilateral interconnected network of sex-steroid responsive neurons in the arcuate nucleus of the rat that coexpress NKB, kisspeptin, dynorphin and ERα and project to GnRH terminals in the median eminence. The importance of the NK3 receptor in this network is underscored by its presence both on arcuate NKB neurons (Burke et al., 2006) and GnRH terminals in the median eminence (Krajewski et al., 2005b). GnRH secretion is pulsatile and this pattern is essential for the regulation of pituitary responsiveness, follicular development and ovarian steroid secretion (Belchetz et al., 1978). Moreover, electrophysiological recordings in the arcuate nucleus of the monkey (Wilson et al., 1984), goat (Maeda et al., 1995) and rat (Kimura et al., 1991; Kinsey-Jones et al., 2008) have revealed volleys of multiunit activity that are timed with pulses of LH in peripheral plasma. Recent studies have emphasized the inherent pulsatility of GnRH neurons (Moenter et al., 2003) with a network of interconnected dendrites to synchronize activity (Campbell et al., 2009). Synchronization mechanisms have also been postulated to take place at the level of GnRH terminals in the median eminence (Moenter et al., 2003; Herbison, 2006). Inputs to the GnRH network at the level of the median eminence would also need to be coordinated to ensure that secretion remains pulsatile. Connections among the NKB/kisspeptin/dynorphin/ERα neurons within the arcuate nucleus provides an anatomic framework to explain how these neurons could be coordinated bilaterally to provide sex-steroid modulation of pulsatile GnRH secretion.

From the arcuate nucleus, NKB/kisspeptin/dynorphin neurons project dorsally and rostrally via a periventricular hypothalamic pathway and laterally through the ventral hypothalamic tract. These projections could also influence the reproductive axis. Arcuate NKB-ir neurons project to the rostral periventricular area of the third ventricle and AVPV consistent with previous anterograde and retrograde-tract tracing studies (Bouret et al., 2004; Hahn and Coen, 2006). The AVPV and rostral periventricular area play critical roles in estrogen positive feedback and the generation of the LH surge in the rodent (Simerly, 1998; Petersen et al., 2003; Clarkson et al., 2008; Herbison, 2008). These regions coexpress kisspeptin and ERα (Smith et al., 2005; Clarkson et al., 2008) and directly project to GnRH neurons (Wintermantel et al., 2006). We also describe projections of the arcuate NKB neurons to the dorsomedial nucleus, a site of gonadotropin inhibitory neurons (Kriegsfeld et al., 2006; Rizwan et al., 2009). Finally, arcuate NKB neurons project to the medial preoptic nucleus, medial preoptic area and septal regions, consistent with previous retrograde tract-tracing studies (Simonian et al., 1999; Hahn and Coen, 2006). These areas have been implicated in the control of reproductive behavior (Pfaff et al., 2006) and are the site of GnRH cell bodies (Barry et al., 1985). However, with the exception of NKB-ir neurons within the arcuate, the cellular identity of the specific cell types that are contacted by projections of arcuate NKB-ir neurons remains to be determined. The influence of arcuate NKB/kisspeptin/dynorphin neurons will also depend on multiple factors, such as the relative coexpression of the peptides in secretory vesicles, the

presence of classical neurotransmitters such as glutamate (Ciofi et al., 2006) and the expression of receptors in the target areas.

The multiple projections of arcuate NKB/kisspeptin/dynorphin neurons suggest that these sex-steroid responsive neurons could also participate in the regulation of numerous homeostatic, behavioral and neuroendocrine circuits. For example, fluid balance and cardiovascular function could be modulated through projections to the paraventricular nucleus (Haley and Flynn, 2008) or periventricluar hypothalamus (Saper and Levisohn, 1983; McKinley et al., 2001). Projections to the paraventricular nucleus could also play a role in feeding, the stress response and autonomic regulation (Simerly, 2004). Arcuate NKB/kisspeptin/dynorphin neurons could influence thermoregulation via projections to the medial preoptic nucleus, dorsomedial nucleus, median preoptic nucleus, septal nuclei or the periventricular projection pathway (Griffin et al., 2001; Romanovsky, 2007). Anterior pituitary function could be modulated via inputs to neuroendocrine neurons within the arcuate nucleus (Krajewski et al., 2005b) and projections to other arcuate neurons could modulate ingestive behavior and energy balance. Thus, in addition to the essential role in the regulation of GnRH secretion, NKB/kisspeptin/dynorphin neurons could relay information from sex-steroids to optimize the internal milieu for reproduction. This concept is in line with our understanding of the arcuate nucleus as a key player in a variety of homeostatic circuits and neuroendocrine functions (Chronwall, 1985). The essential nature of NKB and kisspeptin receptor signaling for the propagation of the species underscores the importance of understanding the anatomic connections and function of NKB/kisspeptin/dynorphin neurons in the arcuate nucleus.

Acknowledgments

The authors thank Penny Dacks, Melinda Smith and Marina Cholanian for careful comments this manuscript. We also acknowledge the University of Virginia Center for Research in Reproduction Ligand Assay and Analysis Core supported by the Eunice Kennedy Shriver NICHD/NIH Grant U54-HD28934) for the hormone assays.

Grant Sponsor: NIH R01 AG-09214 and AG-032315

References

Abel TW, Voytko ML, Rance NE. The effects of hormone replacement therapy on hypothalamic neuropeptide gene expression in a primate model of menopause. J Clin Endocrinol Metab 1999;84:2111–2118. [PubMed: 10372719]

Adachi S, Yamada S, Takatsu Y, Matsui H, Kinoshita M, Takase K, Sugiura H, Ohtaki T, Matsumoto H, Uenoyama Y, Tsukamura H, Inoue K, Maeda K. Involvement of anteroventral periventricular metastin/kisspeptin neurons in estrogen positive feedback action on luteinizing hormone release in female rats. J Reprod Dev 2007;53:367–378. [PubMed: 17213691]

Amstalden M, Coolen LM, Hemmerle AM, Billings HJ, Connors JM, Goodman RL, Lehman MN. Neurokinin 3 receptor immunoreactivity in the septal region, preoptic area and hypothalamus of the female sheep: colocalization in neurokinin B Cells of the arcuate nucleus but not in gonadotrophin-releasing hormone neurones. J Neuroendocrinol. 2009 In press.

Badger TM, Millard WJ, Martin JB, Rosenblum PM, Levenson SE. Hypothalamic-pituitary function in adult rats treated neonatally with monosodium glutamate. Endocrinology 1982;111:2031–2038. [PubMed: 6754352]

Barry, J.; Hoffman, GE.; Wray, S. LHRH-containing systems. In: Björklund, A.; Hökfelt, T., editors. Handbook of Chemical Neuroanatomy Vol 4 GABA and neuropeptides in the CNS Part I. Amsterdam: Elsevier Science; 1985. p. 166-215.

Belchetz PE, Plant TM, Nakai Y, Keogh EJ, Knobil E. Hypophysial responses to continuous and intermittent delivery of hypothalamic gonadotropin-releasing hormone. Science 1978;202:631–633. [PubMed: 100883]

Bouret SG, Draper SJ, Simerly RB. Formation of projection pathways from the arcuate nucleus of the hypothalamus to hypothalamic regions implicated in the neural control of feeding behavior in mice. J Neurosci 2004;24:2797–2805. [PubMed: 15028773]

Burke MC, Letts PA, Krajewski SJ, Rance NE. Coexpression of dynorphin and neurokinin B immunoreactivity in the rat hypothalamus: morphologic evidence of interrelated function within the arcuate nucleus. J Comp Neurol 2006;498:712–726. [PubMed: 16917850]

Campbell RE, Gaidamaka G, Han SK, Herbison AE. Dendro-dendritic bundling and shared synapses between gonadotropin-releasing hormone neurons. Proc Natl Acad Sci U S A 2009;106:10835–10840. [PubMed: 19541658]

Caraty A, Fabre-Nys C, Delaleu B, Locatelli A, Bruneau G, Karsch FJ, Herbison A. Evidence that the mediobasal hypothalamus is the primary site of action of estradiol in inducing the preovulatory gonadotropin releasing hormone surge in the ewe. Endocrinology 1998;139:1752–1760. [PubMed: 9528959]

Chronwall BM. Anatomy and physiology of the neuroendocrine arcuate nucleus. Peptides 1985;6(Suppl 2):1–11. [PubMed: 2417205]

Ciofi P, Krause JE, Prins GS, Mazzuca M. Presence of nuclear androgen receptor-like immunoreactivity in neurokinin B-containing neurons of the hypothalamic arcuate nucleus of the adult male rat. Neurosci Lett 1994;182:193–196. [PubMed: 7715808]

Ciofi P, Leroy D, Tramu G. Sexual dimorphism in the organization of the rat hypothalamic infundibular area. Neuroscience 2006;141:1731–1745. [PubMed: 16809008]

Clarkson J, d'Anglemont de Tassigny X, Moreno AS, Colledge WH, Herbison AE. Kisspeptin-GPR54 signaling is essential for preovulatory gonadotropin-releasing hormone neuron activation and the luteinizing hormone surge. J Neurosci 2008;28:8691–8697. [PubMed: 18753370]

Clemens JA, Roush ME, Fuller RW, Shaar CJ. Changes in luteinizing hormone and prolactin control mechanisms produced by glutamate lesions of the arcuate nucleus. Endocrinology 1978;103:1304–1312. [PubMed: 33802]

Couse JF, Yates MM, Walker VR, Korach KS. Characterization of the hypothalamic-pituitary-gonadal axis in estrogen receptor (ER) null mice reveals hypergonadism and endocrine sex reversal in females lacking ERα but not ERβ. Mol Endocrinol 2003;17:1039–1053. [PubMed: 12624116]

Danzer SC, Price RO, McMullen NT, Rance NE. Sex steroid modulation of neurokinin B gene expression in the arcuate nucleus of adult male rats. Mol Brain Res 1999;66:200–204. [PubMed: 10095095]

de Roux N, Genin E, Carel JC, Matsuda F, Chaussain JL, Milgrom E. Hypogonadotropic hypogonadism due to loss of function of the KiSS1-derived peptide receptor GPR54. Proc Natl Acad Sci U S A 2003;100:10972–10976. [PubMed: 12944565]

Dellovade TL, Merchenthaler I. Estrogen regulation of neurokinin B gene expression in the mouse arcuate nucleus is mediated by estrogen receptor α. Endocrinology 2004;145:736–742. [PubMed: 14592957]

Dorling AA, Todman MG, Korach KS, Herbison AE. Critical role for estrogen receptor alpha in negative feedback regulation of gonadotropin-releasing hormone mRNA expression in the female mouse. Neuroendocrinology 2003;78:204–209. [PubMed: 14583652]

Estrada KM, Clay CM, Pompolo S, Smith JT, Clarke IJ. Elevated KiSS-1 expression in the arcuate nucleus prior to the cyclic preovulatory gonadotrophin-releasing hormone/lutenising hormone surge in the ewe suggests a stimulatory role for kisspeptin in oestrogen-positive feedback. J Neuroendocrinol 2006;18:806–809. [PubMed: 16965299]

Foradori CD, Amstalden M, Goodman RL, Lehman MN. Colocalisation of dynorphin A and neurokinin B immunoreactivity in the arcuate nucleus and median eminence of the sheep. J Neuroendocrinol 2006;18:534–541. [PubMed: 16774502]

Goodman RL, Coolen LM, Anderson GM, Hardy SL, Valent M, Connors JM, Fitzgerald ME, Lehman MN. Evidence that dynorphin plays a major role in mediating progesterone negative feedback on gonadotropin-releasing hormone neurons in sheep. Endocrinology 2004;145:2959–2967. [PubMed: 14988383]

Goodman RL, Lehman MN, Smith JT, Coolen LM, de Oliveira CVR, Jafarzadehshirazi MR, Pereira A, Iqbal J, Caraty A, Ciofi P, Clarke IJ. Kisspeptin neurons in the arcuate nucleus of the ewe express both dynorphin A and neurokinin B. Endocrinology 2007;148:5752–5760. [PubMed: 17823266]

Greeley GH Jr, Nicholson GF, Nemeroff CB, Youngblood WW, Kizer JS. Direct evidence that the arcuate nucleus-median eminence tuberoinfundibular system is not of primary importance in the feedback regulation of luteinizing hormone and follicle-stimulating hormone secretion in the castrated rat. Endocrinology 1978;103:170–175. [PubMed: 744070]

Griffin JD, Saper CB, Boulant JA. Synaptic and morphological characteristics of temperature-sensitive and -insensitive rat hypothalamic neurones. J Physiol 2001;537:521–535. [PubMed: 11731583]

Hahn JD, Coen CW. Comparative study of the sources of neuronal projections to the site of gonadotrophin-releasing hormone perikarya and to the anteroventral periventricular nucleus in female rats. J Comp Neurol 2006;494:190–214. [PubMed: 16304687]

Haley GE, Flynn FW. Blockade of NK3R signaling in the PVN decreases vasopressin and oxytocin release and c-Fos expression in the magnocellular neurons in response to hypotension. Am J Physiol Regul Integr Comp Physiol 2008;295:R1158–R1167. [PubMed: 18650316]

Herbison, AE. Physiology of the gonadotropin-releasing hormone neuronal network. In: Neill, JD.; Plant, TM.; Pfaff, DW.; Challis, JRG.; de Kretser, DM.; Richards, JS.; Wassarman, PM., editors. Knobil and Neill's Physiology of Reproduction. Third. Elsevier; 2006. p. 1415-1482.

Herbison AE. Estrogen positive feedback to gonadotropin-releasing hormone (GnRH) neurons in the rodent: the case for the rostral periventricular area of the third ventricle (RP3V). Brain Res Rev 2008;57:277–287. [PubMed: 17604108]

Jennes L, Stumpf WE, Bissette G, Nemeroff CB. Monosodium glutamate lesions in rat hypothalamus studied by immunohistochemistry for gonadotropin releasing hormone, neurotensin, tyrosine hydroxylase, and glutamic acid decarboxylase and by autoradiography for [3H] estradiol. Brain Res 1984;308:245–253. [PubMed: 6148123]

Kimura F, Nishihara M, Hiruma H, Funabashi T. Naloxone increases the frequency of the electrical activity of luteinizing hormone-releasing hormone pulse generator in long- term ovariectomized rats. Neuroendocrinology 1991;53:97–102. [PubMed: 2046864]

Kinsey-Jones JS, Li XF, Luckman SM, O'Byrne KT. Effects of kisspeptin-10 on the electrophysiological manifestation of gonadotropin-releasing hormone pulse generator activity in the female rat. Endocrinology 2008;149:1004–1008. [PubMed: 18063679]

Kirigiti MA, True C, Ciofi PGKL, Smith MS. Kisspeptin and NKB fiber distribution in the adult female rat: relationship to GnRH cell bodies and fibers/terminals in the median eminence. Endocrine Society Abstract 2009:3–223.

Krajewski SJ, Anderson MJ, Burke MC, McMullen NT, Rance NE. Arcuate neurokinin B neurons project to the median eminence as well as multiple hypothalamic sites: an anterograde tract-tracing study using biotinylated dextran amine. Soc Neurosci Abstr 2005a;31:760.7.

Krajewski SJ, Anderson MJ, Iles-Shih L, Chen KJ, Urbanski HF, Rance NE. Morphologic evidence that neurokinin B modulates gonadotropin-releasing hormone secretion via neurokinin 3 receptors in the rat median eminence. J Comp Neurol 2005b;489:372–386. [PubMed: 16025449]

Krajewski SJ, Burke MC, McMullen NT, Rance NE. Projections of arcuate neurokinin B neurons in the rat hypothalamus: a study using neonatal ablation of the arcuate nucleus by monosodium l-glutamate. Soc Neurosci Abstr 2008;34:185.16.

Kriegsfeld LJ, Mei DF, Bentley GE, Ubuka T, Mason AO, Inoue K, Ukena K, Tsutsui K, Silver R. Identification and characterization of a gonadotropin-inhibitory system in the brains of mammals. Proc Natl Acad Sci U S A 2006;103:2410–2415. [PubMed: 16467147]

Lucas LR, Hurley DL, Krause JE, Harlan RE. Localization of the tachykinin neurokinin B precursor peptide in rat brain by immunocytochemistry and *in situ* hybridization. Neuroscience 1992;51:317–345. [PubMed: 1465196]

Maeda KI, Tsukamura H, Ohkura S, Kawakami S, Nagabukuro H, Yokoyama A. The LHRH pulse generator: a mediobasal hypothalamic location. Neurosci Biobehav Rev 1995;19:427–437. [PubMed: 7566744]

Marksteiner J, Sperk G, Krause JE. Distribution of neurons expressing neurokinin B in the rat brain: immunohistochemistry and in situ hybridization. J Comp Neurol 1992;317:341–356. [PubMed: 1374442]

McKinley MJ, Allen AM, May CN, McAllen RM, Oldfield BJ, Sly D, Mendelsohn FAO. Neural pathways from the lamina terminalis influencing cardiovascular and body fluid homeostasis. Clin Exp Pharmacol Physiol 2001;28:990–992. [PubMed: 11903300]

Meister B, Ceccatelli S, Hökfelt T, Andén NE, Andén M, Theodorsson E. Neurotransmitters, neuropeptides and binding sites in the rat mediobasal hypothalamus: effects of monosodium glutamate (MSG) lesions. Exp Brain Res 1989;76:343–368. [PubMed: 2569986]

Merchenthaler I, Maderdrut JL, O'Harte F, Conlon JM. Localization of neurokinin B in the central nervous system of the rat. Peptides 1992;13:815–829. [PubMed: 1437720]

Merighi A. Costorage and coexistence of neuropeptides in the mammalian CNS. Prog Neurobiol 2002;66:161–190. [PubMed: 11943450]

Moenter SM, DeFazio RA, Pitts GR, Nunemaker CS. Mechanisms underlying episodic gonadotropin-releasing hormone secretion. Front Neuroendocrinol 2003;24:79–93. [PubMed: 12762999]

Navarro VM, Gottsch ML, Chavkin C, Okamura H, Clifton DK, Steiner RA. Regulation of Gonadotropin-Releasing Hormone Secretion by Kisspeptin/Dynorphin/Neurokinin B Neurons in the Arcuate Nucleus of the Mouse. J Neurosci 2009;29:11859–11866. [PubMed: 19776272]

Nemeroff CB, Lipton MA, Kizer JS. Models of neuroendocrine regulation: use of monosodium glutamate as an investigational tool. Dev Neurosci 1978;1:102–109. [PubMed: 39735]

Olney JW. Brain lesions, obesity, and other disturbances in mice treated with monosodium glutamate. Science 1969;164:719–721. [PubMed: 5778021]

Paxinos, G.; Watson, C. The rat brain in stereotaxic coordinates. Burlington, MA: Elsevier Inc.; 2007.

Petersen SL, Ottem EN, Carpenter CD. Direct and indirect regulation of gonadotropin-releasing hormone neurons by estradiol. Biol Reprod 2003;69:1771–1778. [PubMed: 12890720]

Pfaff, DW.; Sakuma, Y.; Kow, LM.; Lee, AW.; Easton, A. Hormonal, neuronal and genomic mechanisms for female reproductive behaviors, motivation and arousal. In: Neill, JD.; Plant, TM.; Pfaff, DW.; Challis, JRG.; de Kretser, DM.; Richards, JS.; Wassarman, PM., editors. Knobil and Neill's Physiology of Reproduction. Third. Elsievier; 2006. p. 1825-1920.

Pillon D, Caraty A, Fabre-Nys C, Bruneau G. Short-term effect of oestradiol on neurokinin B mRNA expression in the infundibular nucleus of ewes. J Neuroendocrinol 2003;15:749–753. [PubMed: 12834435]

Ramaswamy S, Guerriero KA, Gibbs RB, Plant TM. Structural interactions between kisspeptin and GnRH neurons in the mediobasal hypothalamus of the male rhesus monkey (*Macaca mulatta*) as revealed by double immunofluorescence and confocal microscopy. Endocrinology 2008;149:4387–4395. [PubMed: 18511511]

Rance NE. Menopause and the human hypothalamus: evidence for the role of kisspeptin/neurokinin B neurons in the regulation of estrogen negative feedback. Peptides 2009;30:111–122. [PubMed: 18614256]

Rance NE, Bruce TR. Neurokinin B gene expression is increased in the arcuate nucleus of ovariectomized rats. Neuroendocrinology 1994;60:337–345. [PubMed: 7529897]

Rance NE, McMullen NT, Smialek JE, Price DL, Young WS III. Postmenopausal hypertrophy of neurons expressing the estrogen receptor gene in the human hypothalamus. J Clin Endocrinol Metab 1990;71:79–85. [PubMed: 2370302]

Rance NE, Young WS III. Hypertrophy and increased gene expression of neurons containing neurokinin-B and substance-P messenger ribonucleic acids in the hypothalami of postmenopausal women. Endocrinology 1991;128:2239–2247. [PubMed: 1708331]

Reiner A, Veenman CL, Medina L, Jiao Y, Del Mar N, Honig MG. Pathway tracing using biotinylated dextran amines. J Neurosci Methods 2000;103:23–37. [PubMed: 11074093]

Rizwan MZ, Porteous R, Herbison AE, Anderson GM. Cells expressing RFamide-related peptide-1/3, the mammalian gonadotropin-inhibitory hormone orthologs, are not hypophysiotropic neuroendocrine neurons in the rat. Endocrinology 2009;150:1413–1420. [PubMed: 19008316]

Romanovsky AA. Thermoregulation: some concepts have changed. Functional architecture of the thermoregulatory system. Am J Physiol Regul Integr Comp Physiol 2007;292:R37–R46. [PubMed: 17008453]

Rometo AM, Krajewski SJ, Voytko ML, Rance NE. Hypertrophy and increased kisspeptin gene expression in the hypothalamic infundibular nucleus of postmenopausal women and ovariectomized monkeys. J Clin Endocrinol Metab 2007;92:2744–2750. [PubMed: 17488799]

Rometo AM, Rance NE. Changes in prodynorphin gene expression and neuronal morphology in the hypothalamus of postmenopausal women. J Neuroendocrinol 2008;20:1376–1381. [PubMed: 19094085]

Sandoval-Guzmán T, Stalcup ST, Krajewski SJ, Voytko ML, Rance NE. Effects of ovariectomy on the neuroendocrine axes regulating reproduction and energy balance in young cynomolgus macaques. J Neuroendocrinol 2004;16:146–153. [PubMed: 14764001]

Saper CB, Levisohn D. Afferent connections of the median preoptic nucleus in the rat: anatomical evidence for a cardiovascular integrative mechanism in the anteroventral third ventricular (AV3V) region. Brain Res 1983;288:21–31. [PubMed: 6198025]

Seminara SB, Messager S, Chatzidaki EE, Thresher RR, Acierno JS Jr, Shagoury JK, Bo-Abbas Y, Kuohung W, Schwinof KM, Hendrick AG, Zahn D, Dixon J, Kaiser UB, Slaugenhaupt SA, Gusella JF, O'Rahilly S, Carlton MBL, Crowley WF Jr, Aparicio SAJR, Colledge WH. The GPR54 gene as a regulator of puberty. N Engl J Med 2003;349:1614–1627. [PubMed: 14573733]

Seress L. Divergent effects of acute and chronic monosodium l-glutamate treatment on the anterior and posterior parts of the arcuate nucleus. Neuroscience 1982;7:2207–2216. [PubMed: 7145092]

Simerly RB. Organization and regulation of sexually dimorphic neuroendocrine pathways. Behav Brain Res 1998;92:195–203. [PubMed: 9638961]

Simerly, RB. Anatomical substrates of hypothalamic integration. In: Paxinos, G., editor. The Rat Nervous System. Third. Elsevier; Academic Press; 2004. p. 335-368.

Simonian SX, Spratt DP, Herbison AE. Identification and characterization of estrogen receptor α-containing neurons projecting to the vicinity of the gonadotropin-releasing hormone perikarya in the rostral preoptic area of the rat. J Comp Neurol 1999;411:346–358. [PubMed: 10404258]

Smith JT, Clay CM, Caraty A, Clarke IJ. KiSS-1 messenger ribonucleic acid expression in the hypothalamus of the ewe is regulated by sex steroids and season. Endocrinology 2007;148:1150–1157. [PubMed: 17185374]

Smith JT, Cunningham MJ, Rissman EF, Clifton DK, Steiner RA. Regulation of *Kiss*1 gene expression in the brain of the female mouse. Endocrinology 2005;146:3686–3692. [PubMed: 15919741]

Smith JT, Li Q, Pereira A, Clarke IJ. Kisspeptin neurons in the ovine arcuate nucleus and preoptic area are involved in the preovulatory luteinizing hormone surge. Endocrinology 2009;150:5530–5538. [PubMed: 19819940]

Swanson, LW. Brain Maps: Structure of the Rat Brain. Amsterdam: Elsevier; 1992.

Todman MG, Han SK, Herbison AE. Profiling neurotransmitter receptor expression in mouse gonadotropin-releasing hormone neurons using green fluorescent protein-promoter transgenics and microarrays. Neuroscience 2005;132:703–712. [PubMed: 15837132]

Topaloglu AK, Reimann F, Guclu M, Yalin AS, Kotan LD, Porter KM, Serin A, Mungan NO, Cook JR, Ozbek MN, Imamoglu S, Akalin NS, Yuksel B, O'Rahilly S, Semple RK. *TAC3* and *TACR3* mutations in familial hypogonadotropic hypogonadism reveal a key role for Neurokinin B in the central control of reproduction. Nat Genet 2009;2009:354–358. [PubMed: 19079066]

Van den Pol AN, Cassidy JR. The hypothalamic arcuate nucleus of rat - a quantitative Golgi analysis. J Comp Neurol 1982;204:65–98. [PubMed: 7056889]

Warden MK, Young WS III. Distribution of cells containing mRNAs encoding substance P and neurokinin B in the rat central nervous system. J Comp Neurol 1988;272:90–113. [PubMed: 2454979]

Watson RE Jr, Wiegand SJ, Clough RW, Hoffman GE. Use of cryoprotectant to maintain long-term peptide immunoreactivity and tissue morphology. Peptides 1986;7:155–159. [PubMed: 3520509]

Wilson RC, Kesner JS, Kaufman JM, Uemura T, Akema T, Knobil E. Central electrophysiologic correlates of pulsatile luteinizing hormone secretion in the rhesus monkey. Neuroendocrinology 1984;39:256–260. [PubMed: 6504270]

Wintermantel TM, Campbell RE, Porteous R, Bock D, Gröne HJ, Todman MG, Korach KS, Greiner E, Pérez CA, Schütz G, Herbison AE. Definition of estrogen receptor pathway critical for estrogen

positive feedback to gonadotropin-releasing hormone neurons and fertility. Neuron 2006;52:271–280. [PubMed: 17046690]

Abbreviations

3V	third ventricle
ac	anterior commissure
AHA	anterior hypothalamic area
ARC	arcuate nucleus
AVPV	anteroventral periventricular nucleus
BDA	biotinylated dextran amine
BNST	bed nucleus of the stria terminalis
cp	cerebral peduncle
DB	diagonal band
DMN	dorsomedial nucleus
fx	fornix
LHA	lateral hypothalamic area
LPOA	lateral preoptic area
lpz	lateral palisade zone
LSv	ventral portion of the lateral septal nucleus
LV	lateral ventricle
ME	median eminence
MnPO	median preoptic nucleus
MPN	medial preoptic nucleus
MPOA	medial preoptic area
MS	medial septal nucleus
MSG	monosodium glutamate
mtt	mammillothalamic tract
NKB	neurokinin B
oc	optic chiasm
ot	optic tract
OVLT	organum vasculosum of the lamina terminalis
Pe	periventricular hypothalamus
PeFLH	perifornical region of the lateral hypothalamic area
PH	posterior hypothalamus
PVN	paraventricular nucleus
PVN mag	magnocellular division of the paraventricular nucleus
PVN parvi	parvicellular division of the paraventricular nucleus
RCA	retrochiasmatic area

SCN	suprachiasmatic nucleus
SON	supraoptic nucleus
vht	ventral hypothalamic tract
VMN	ventromedial nucleus
vPM	ventral premammillary nucleus

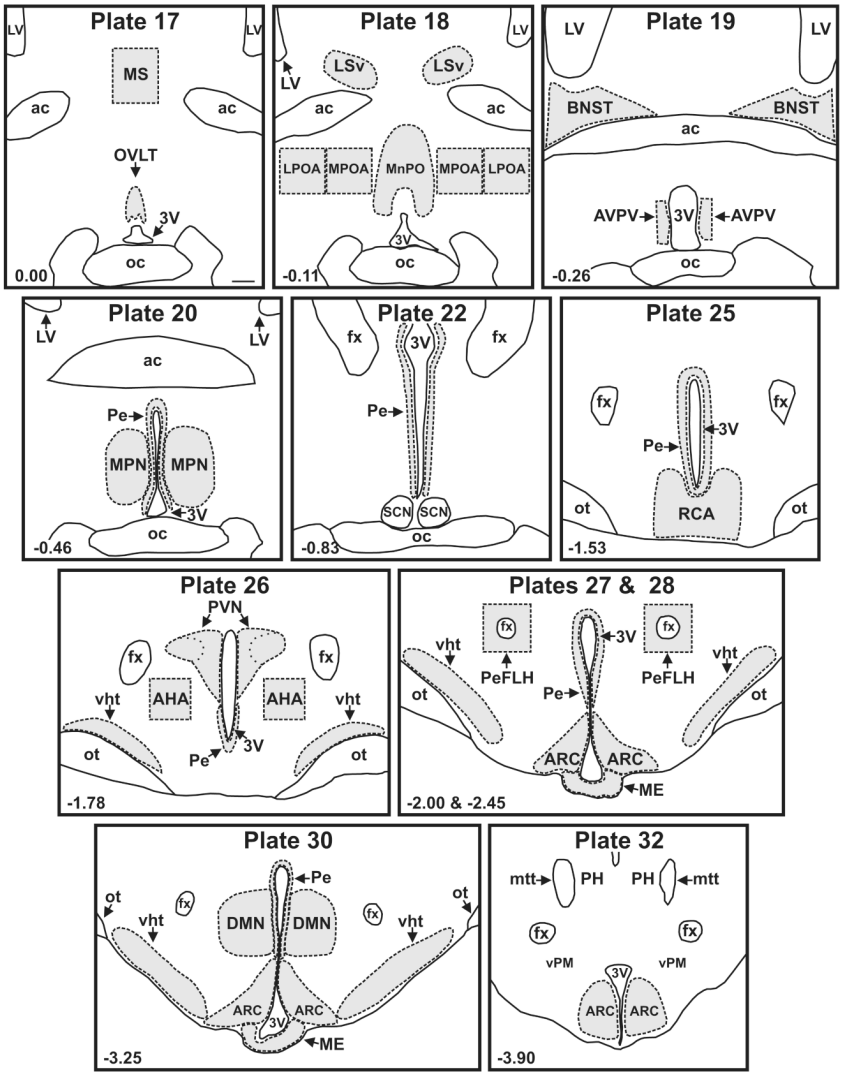

Figure 1.

Line drawings of representative sections from control rats used for analysis of NKB-ir fiber density. Sections were matched to plates in a rat brain atlas listed at the top of each drawing (Swanson, 1992) and regions of interest (shaded areas) were outlined with the aid of the adjacent Nissl-stained sections. The distance from Bregma (mm) is shown in the lower left corner of each map. Scale bar in Plate 17 = 250 μm (applies to all).

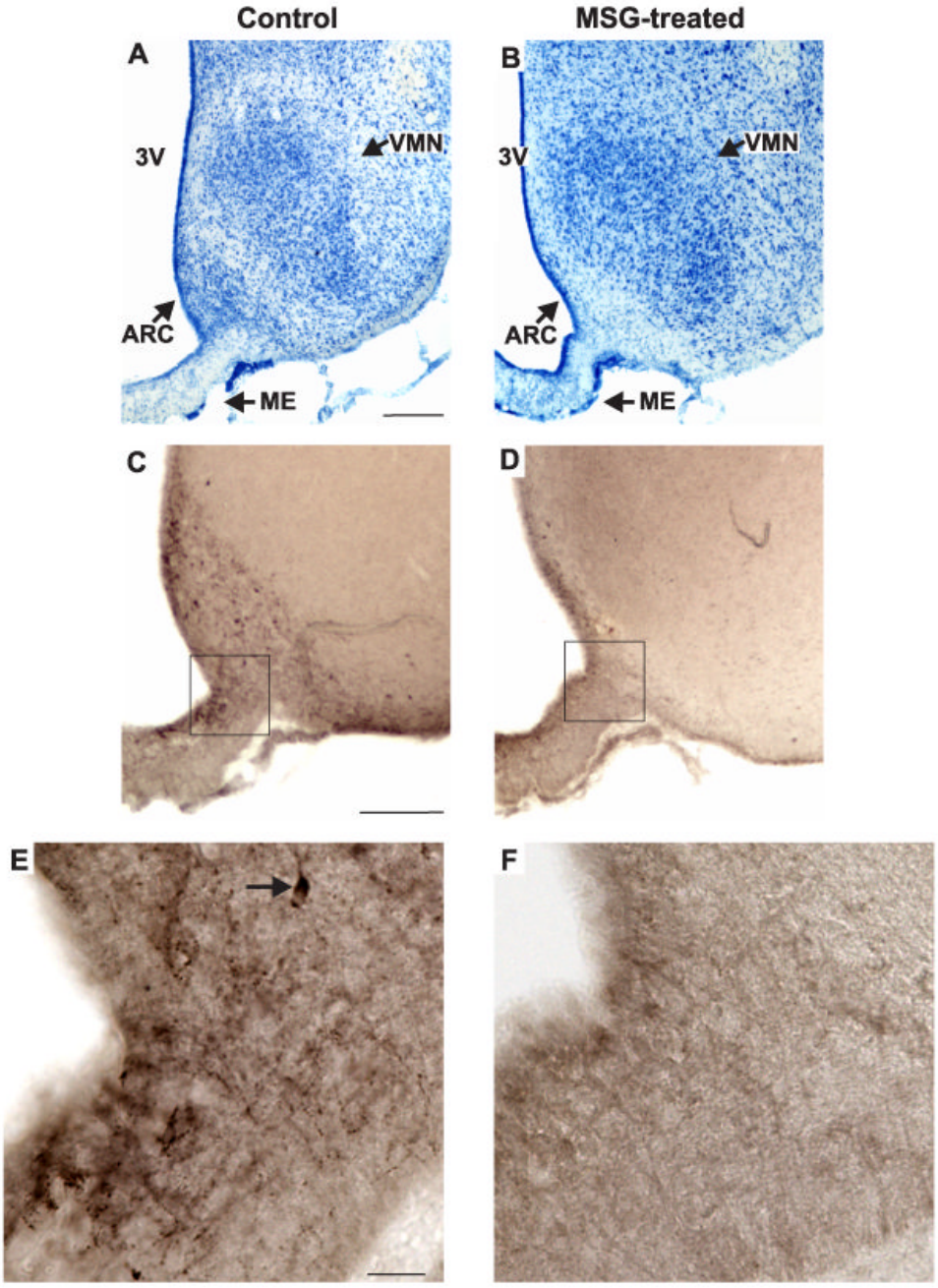

Figure 2.

Representative photomicrographs of adjacent sections in the mid-level of the arcuate nucleus in control (A, C, E) and MSG-treated (B, D, F) rats. (A, B), Methylene blue stain; (C, D, E, F), NKB-immunoreactivity with nickel intensified DAB. The boxes in C and D show the region illustrated in the high magnification photomicrographs of E and F. The Nissl stains from the MSG-treated rats revealed marked degeneration of neurons at most levels of the arcuate nucleus. Immunocytochemical stains confirmed the near-total loss of NKB-ir cells in the arcuate nucleus of MSG-treated animals. The high magnification photomicrographs illustrate loss of cell bodies and fibers in the arcuate nucleus and adjacent median eminence. The arrow

in E points to an NKB-ir somata. Scale bar in A = 250 μm (applies to A and B), Scale bar in C = 200 μm (applies to C and D). Scale bar in E = 25 μm (applies to A-B).

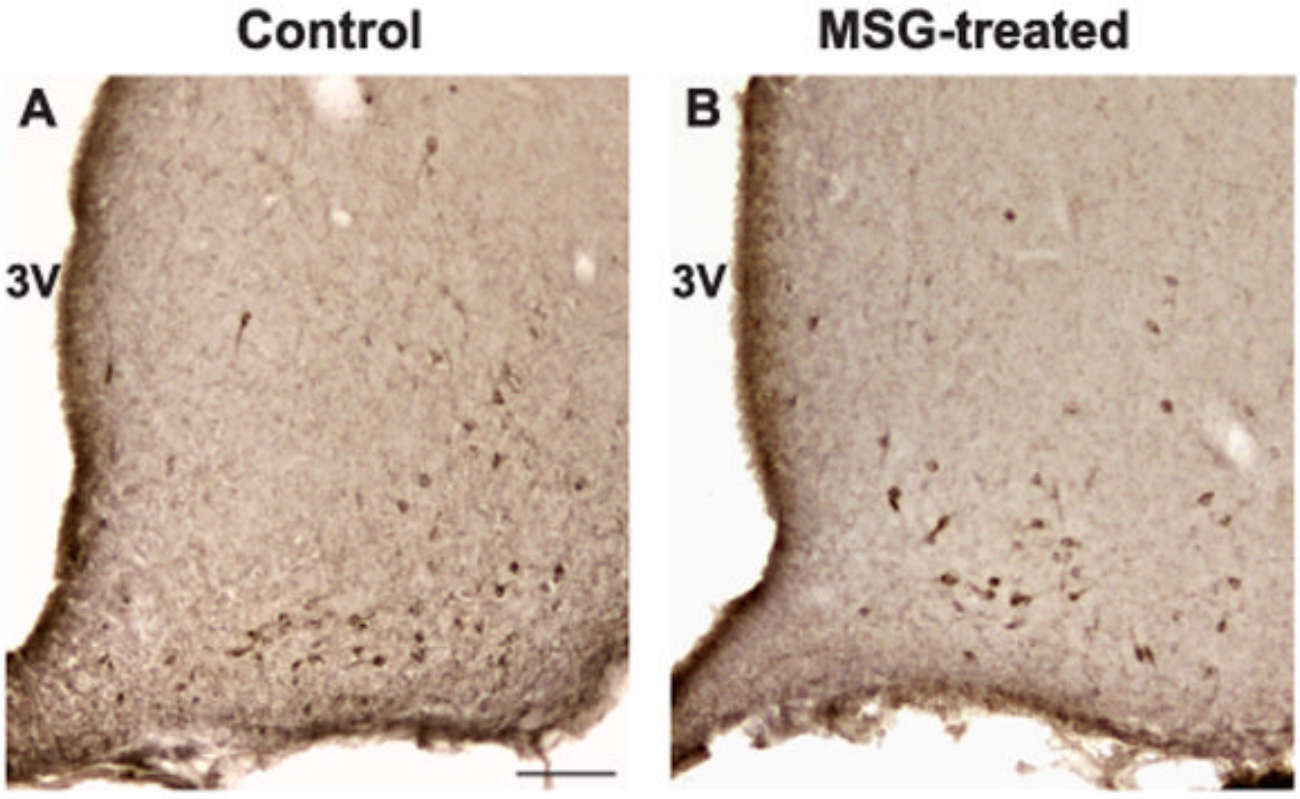

Figure 3.
Representative photomicrographs of NKB-immunoreactivity at the level of the premammillary arcuate nucleus in control (A) and MSG-treated (B) rats. Note the relative preservation of NKB-immunoreactive cell bodies at this level of the arcuate nucleus. Scale bar in A = 100 μm (applies to A and B).

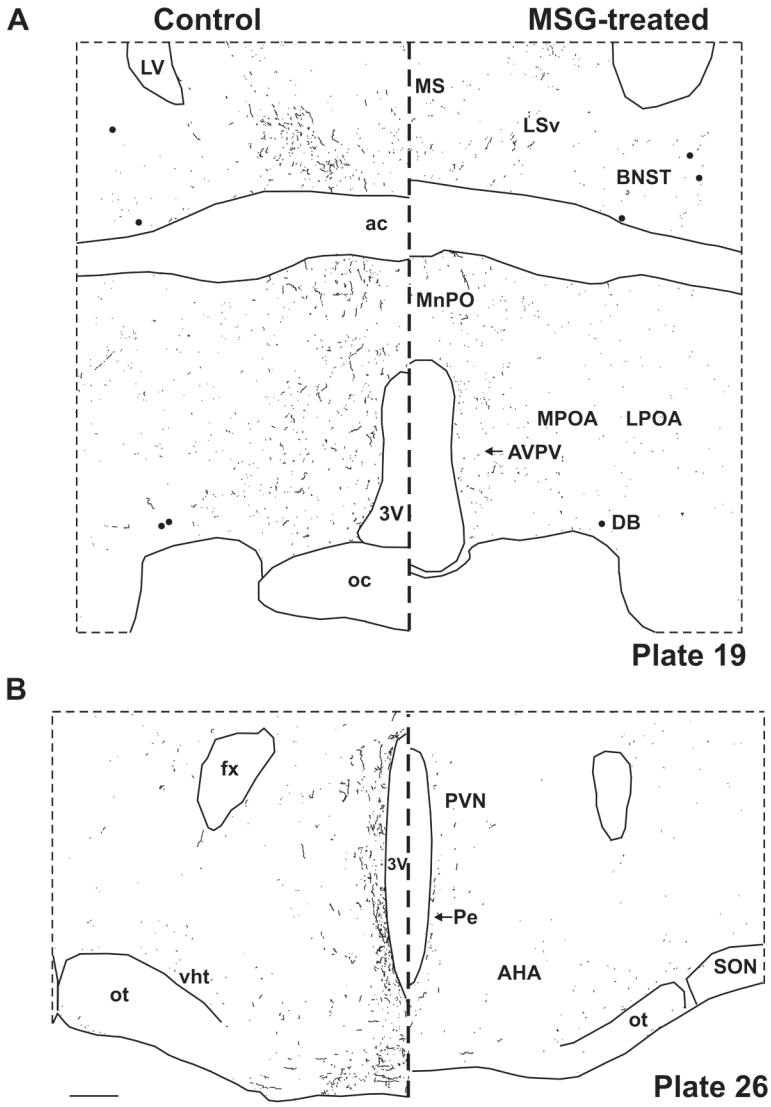

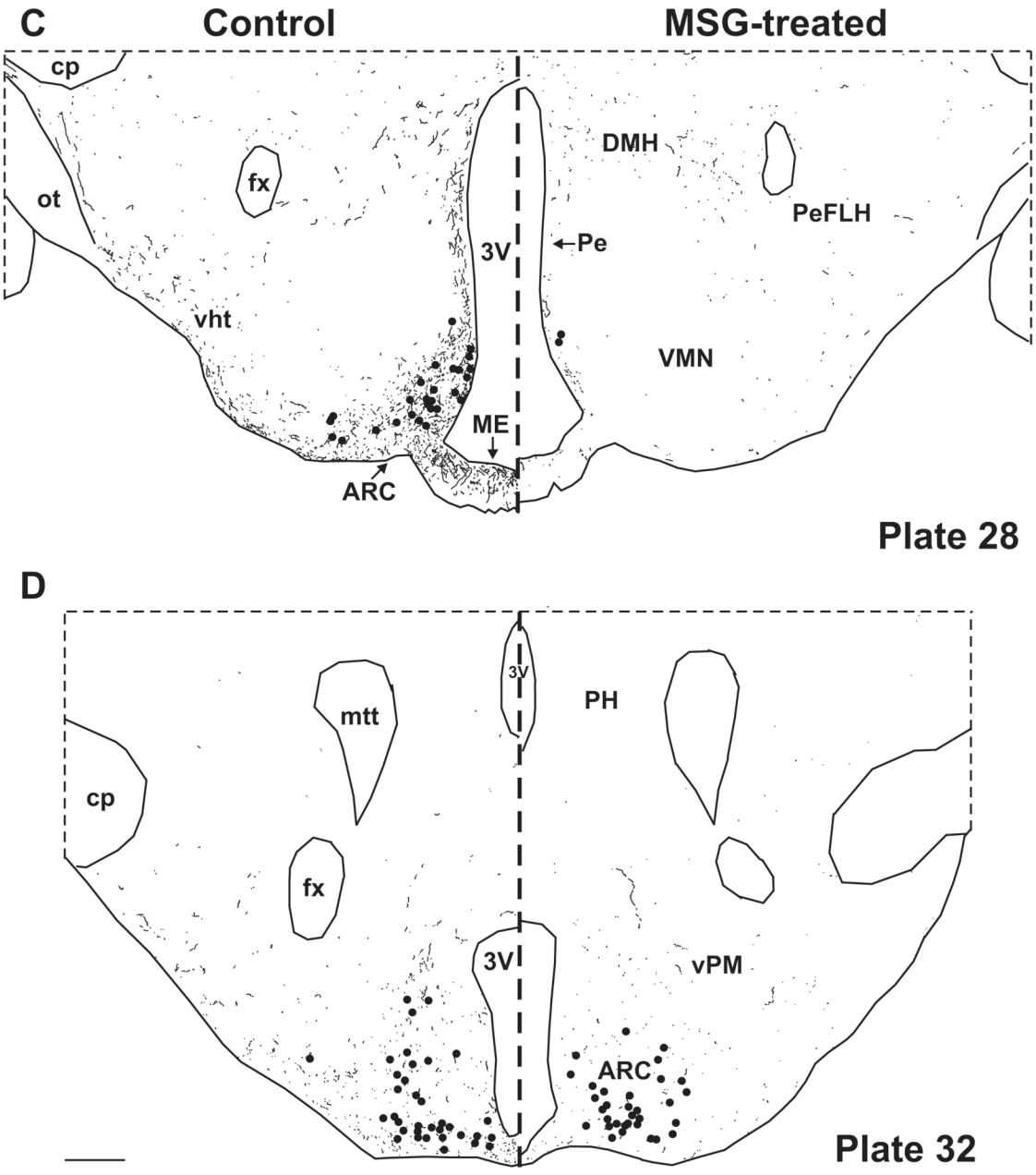

Figure 4.

Computer assisted drawings of NKB-ir neurons (filed circles) and fibers (lines) in control (left) and MSG-treated (right) rats at selected levels of the hypothalamus (A-D). Sections were matched to plates in a rat brain atlas listed in bottom right corner (Swanson, 1992). NKB-ir cells are depleted at most levels of the arcuate nucleus, with near total loss of NKB-ir fibers in the arcuate nucleus and the adjacent median eminence (C). NKB-ir fibers are also reduced in multiple hypothalamic areas (A-D). There is relative preservation of NKB-ir neurons at the level of the premammillary arcuate (D). Scale bars in B and D = 250 μm (applies to all).

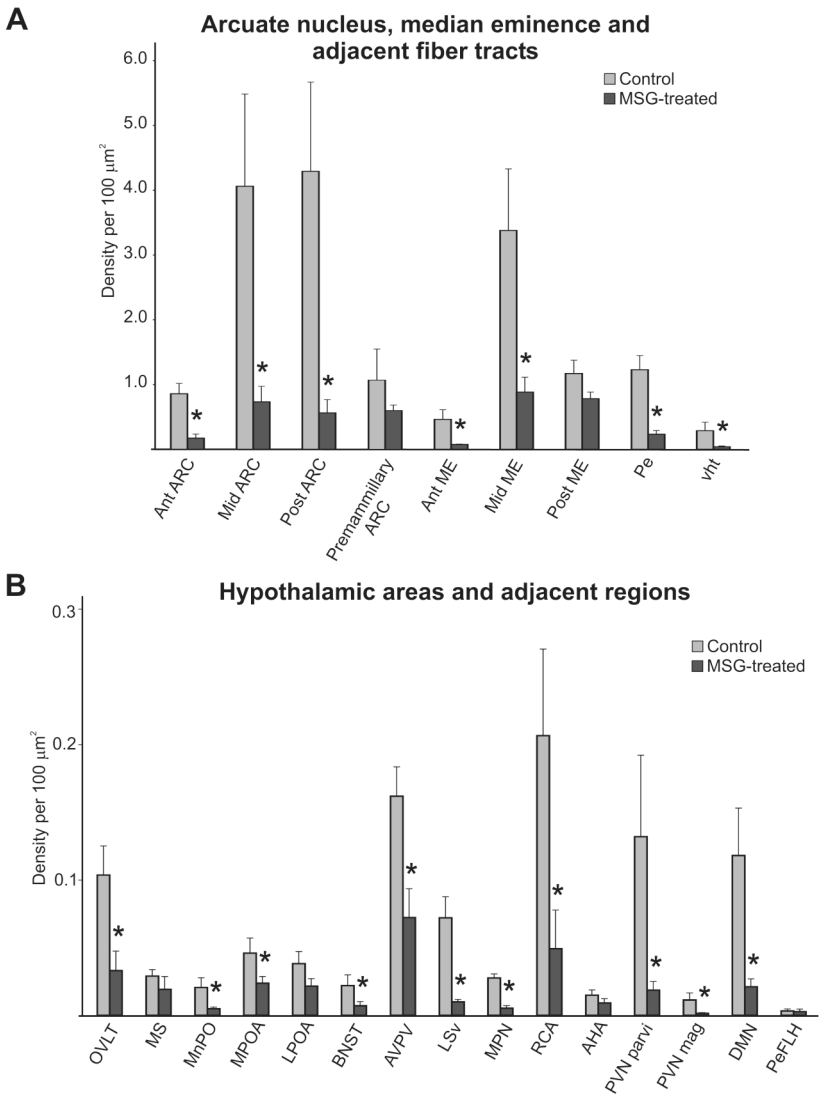

Figure 5.

Bar graphs showing quantitative analysis of NKB-immunoreactivity at multiple levels of the arcuate nucleus, median eminence and fiber tracts (A) and regions throughout the hypothalamus and adjacent areas (B) in control (gray bars) and MSG-treated (black bars) rats. Note the difference in scale between the two graphs indicative of the higher density of NKB-immunoreactivity the arcuate nucleus, median eminence and fiber tracts. Quantitative analysis revealed significantly reduced NKB-immunoreactivity in the arcuate nucleus, median eminence, fiber tracts and multiple hypothalamic areas of MSG-treated rats. n = 3 - 6 animals/group * significantly different from control, $p \leq 0.05$.

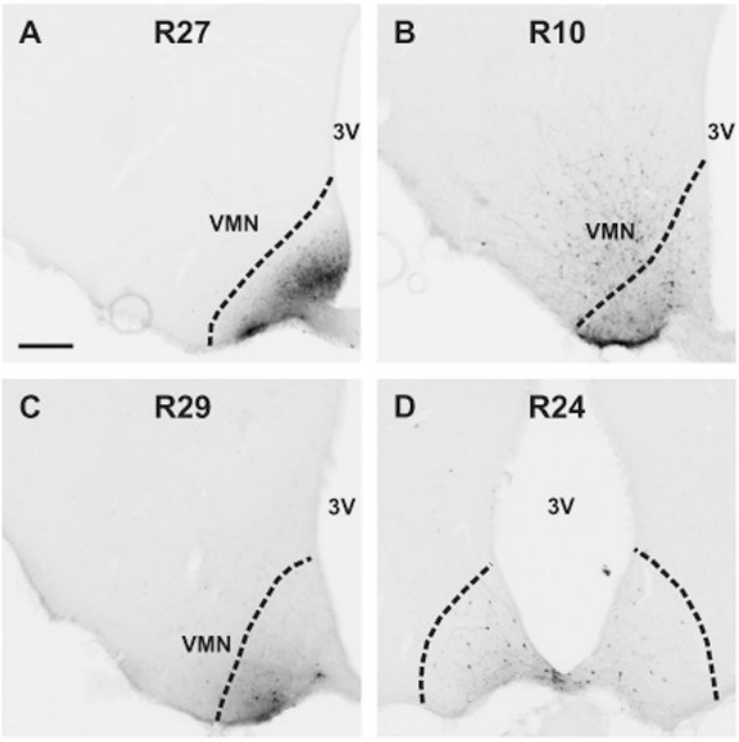

Figure 6.

Photomicrographs of BDA injection sites visualized by avidin-biotin-horseradish peroxidase histochemistry (A-D). The dotted lines indicate the border of the arcuate nucleus. The animal identification number is listed at the top of each photomicrograph. BDA injections were either confined to the arcuate nucleus (A, C, D) or included the arcuate nucleus and adjacent ventromedial nucleus (B). In one animal (D), the injection was midline and BDA was taken up in neurons in on both sides. Two injections (A and B) were at the mid-level of the arcuate nucleus and two (C and D) were in the posterior arcuate nucleus, corresponding to plates 28 (-2.45 from Bregma) and 31 (-3.70 from Bregma), respectively (Swanson, 1992). Scale bar in A = 200 m (applies to all).

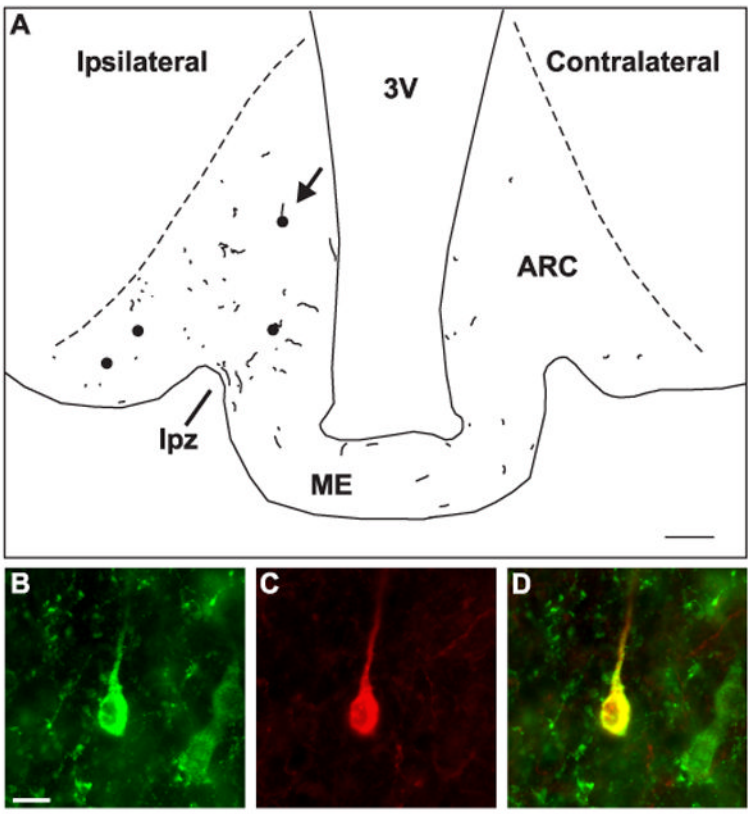

Figure 7.

A) Computer-assisted drawing showing the location of dual-labeled NKB/BDA-ir cell bodies (filled circles) and fibers (lines) near the injection site of R10 (see Fig. 6). This illustration was created by superimposing the tracings from 4 non-adjacent sections. The dotted lines indicate the borders of the arcuate nucleus. The arrow points to the location of the cell illustrated in B-D. Injection of BDA into the arcuate nucleus labeled a small number of NKB-ir neurons in the arcuate nucleus. Antereogradely labeled NKB-ir fibers were identified within the arcuate nucleus and adjacent median eminence including the lateral palisade zone (line). In addition, NKB/BDA-ir fibers were identified across the ME and within the arcuate nucleus of the contralateral side. (B-D) Demonstration of uptake of BDA in a NKB-ir neuron in the arcuate nucleus. High magnification photomicrographs of a NKB-ir cell body (B, green) in the arcuate nucleus that has taken up BDA (C, red). Color-combined image showing co-localization of NKB immunoreactivity and BDA (D, yellow). Scale bar in A = 100 μm. Scale bar in B = 10 μm (applies to B-D).

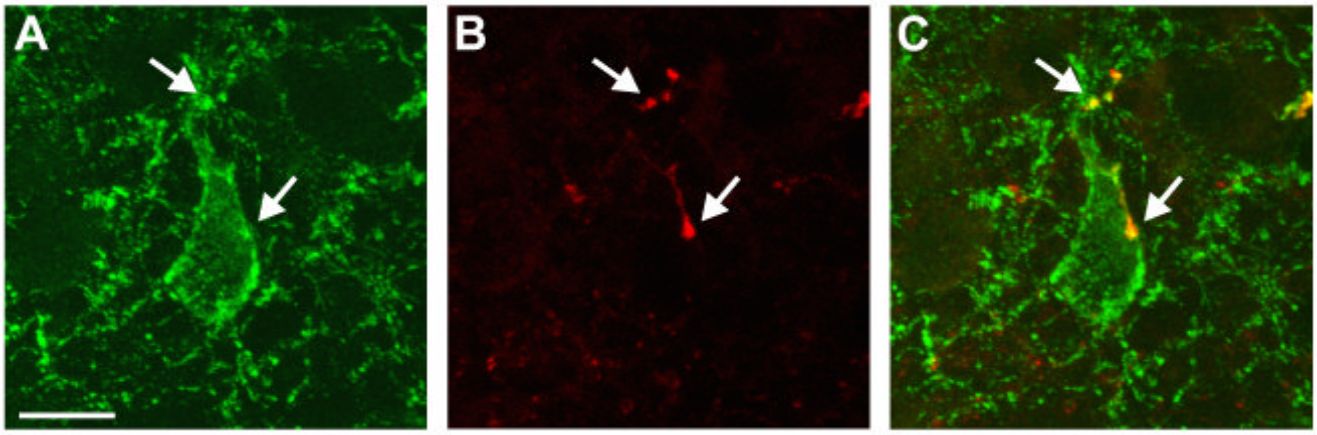

Figure 8.

Confocal microscope projection image of close apposition of a NKB/BDA-ir fiber onto a NKB-ir cell in the arcuate nucleus. NKB immunoreactivity is green (A) and BDA is red (B). The arrows point to dual-labeled fibers (yellow) in close apposition to the somata and proximal dendrite of an NKB-ir neuron ipsilateral to the side of injection. The projection is a stack of seven 0.8 μm thick confocal images. Scale bar in A = 10 μm (applies to all).

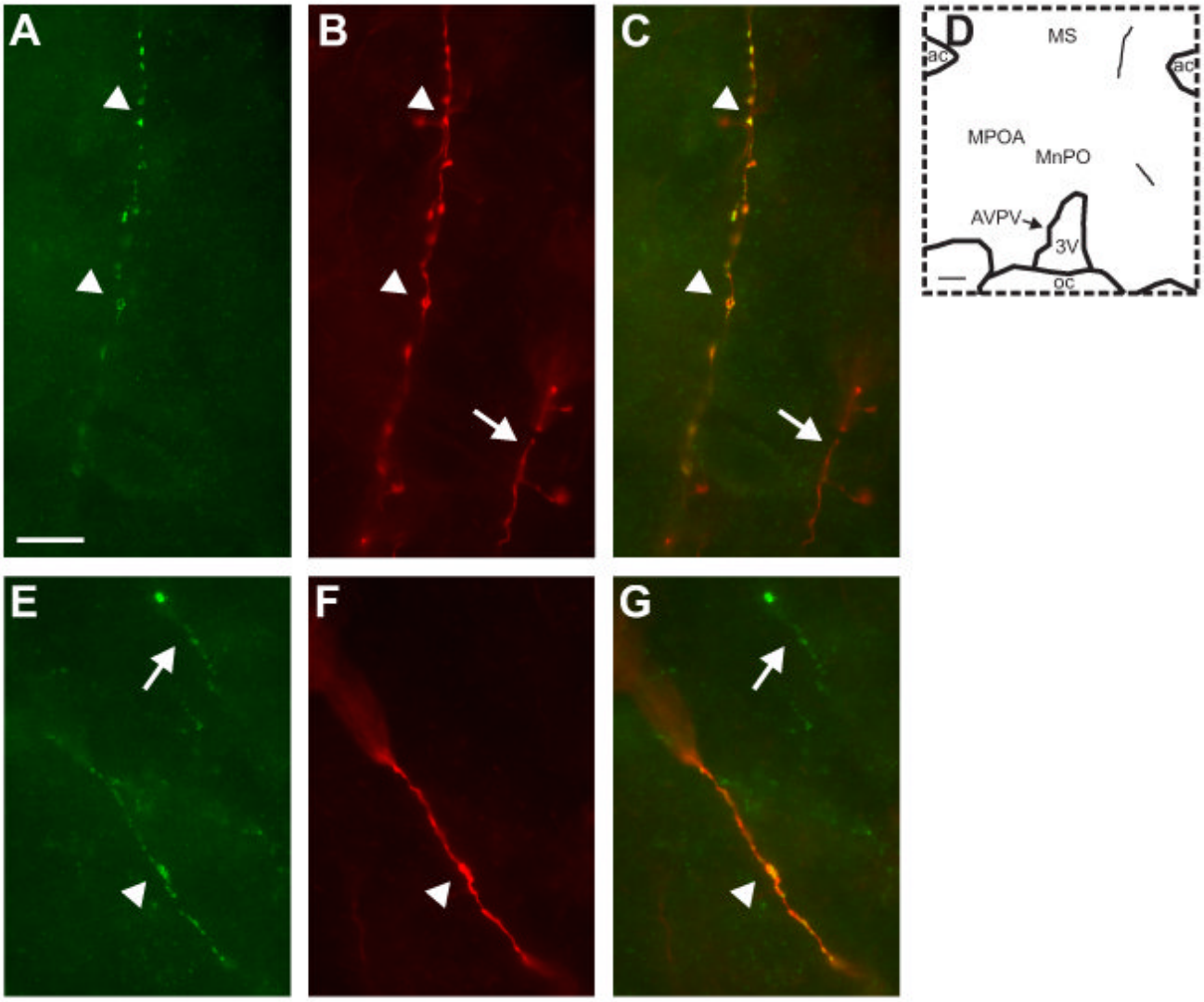

Figure 9.

High magnification photomicrographs of NKB (A and E, green) and BDA (B and F; red) immunofluorescence. The color-combined images (C and G) show that these NKB-immunoreactive axons are anterogradely labeled with BDA (yellow). The map in D shows the location of these dual-labeled axons. The top photomicrographs illustrate a thin, beaded anterogradely-labeled NKB-ir axon extending to the lateral ventral septal region (A, B and C, arrowheads). The bottom photomicrographs illustrate a dual-labeled axon in the medial preoptic region that is thicker and displays few varicosities (E, F, and G, arrowheads). The arrows show single-labeled fibers that are immunoreactive for either BDA (B and C) or NKB (E and G). Scale bar in A = 10 μm (applies to A-C and E-F). Scale bar in D = 200 μm.

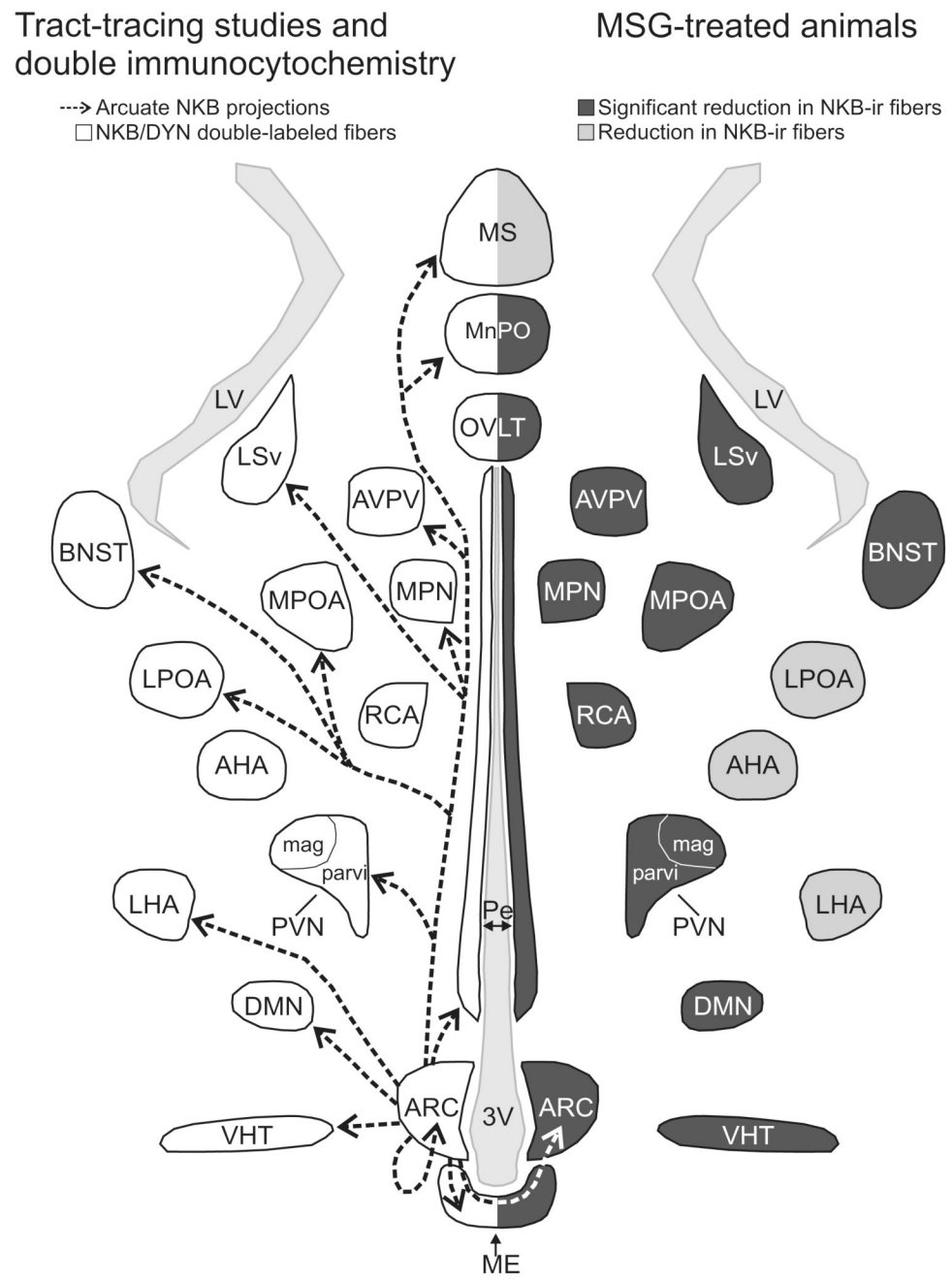

Figure 10.

Schematic diagram (horizontal plane) of arcuate NKB projections revealed by anterograde tract-tracing and NKB/dynorphin immunofluorescence (left) and MSG-ablation of arcuate NKB neurons (right). Left: The arrows indicate the location of arcuate NKB projections labeled by a BDA injection into the arcuate nucleus. The outlined areas show the where dual-labeled NKB/dynorphin-ir fibers were previously described (Burke et al., 2006). Right: The areas shaded in dark gray exhibited a significant reduction in NKB-ir fibers in MSG-treated animals. The areas shaded light gray exhibited a reduction of NKB-ir in MSG-treated animals that was not significantly different. The diverse projections of arcuate NKB neurons provide a

mechanism to integrate the reproductive axis with multiple homeostatic and neuroendocrine circuits.

Table 1

Sites of anterogradely-labeled NKB-ir axons after microinjection of BDA in the arcuate nucleus

	Rat 10	Rat 24	Rat 27	Rat 29
ARC, ipsilateral	X	X	X	X
ARC, contralateral	X	NA	X	
ME	X	X	X	X
Pe	X	X	X	X
vht	X	X	X	X
MS	X	X	X	X
MnPO	X	X		NA
MPOA	X	X	X	
LPOA	X	X	X	
BNST	X	X		
AVPV		NA	X	
LSv	X	X	X	
MPN	X			
PVN, parvicellular	X	X	X	X
DMN		X		
LHA	X	X	X	X

Animal identification numbers are listed at the top (see figure 6). The X marks the regions where NKB/BDA-ir axons were identified in each rat. BDA-ir fibers were also identified in the OVLT, RCA, AHA, SCN, magnocellular PVN, SON and VMN, but none these were immunoreactive for NKB. NA, not analyzed.